iScience

CellPress
OPEN ACCESS

Article

Single-cell RNA sequencing uncovers dynamic roadmap and cell-cell communication during buffalo spermatogenesis

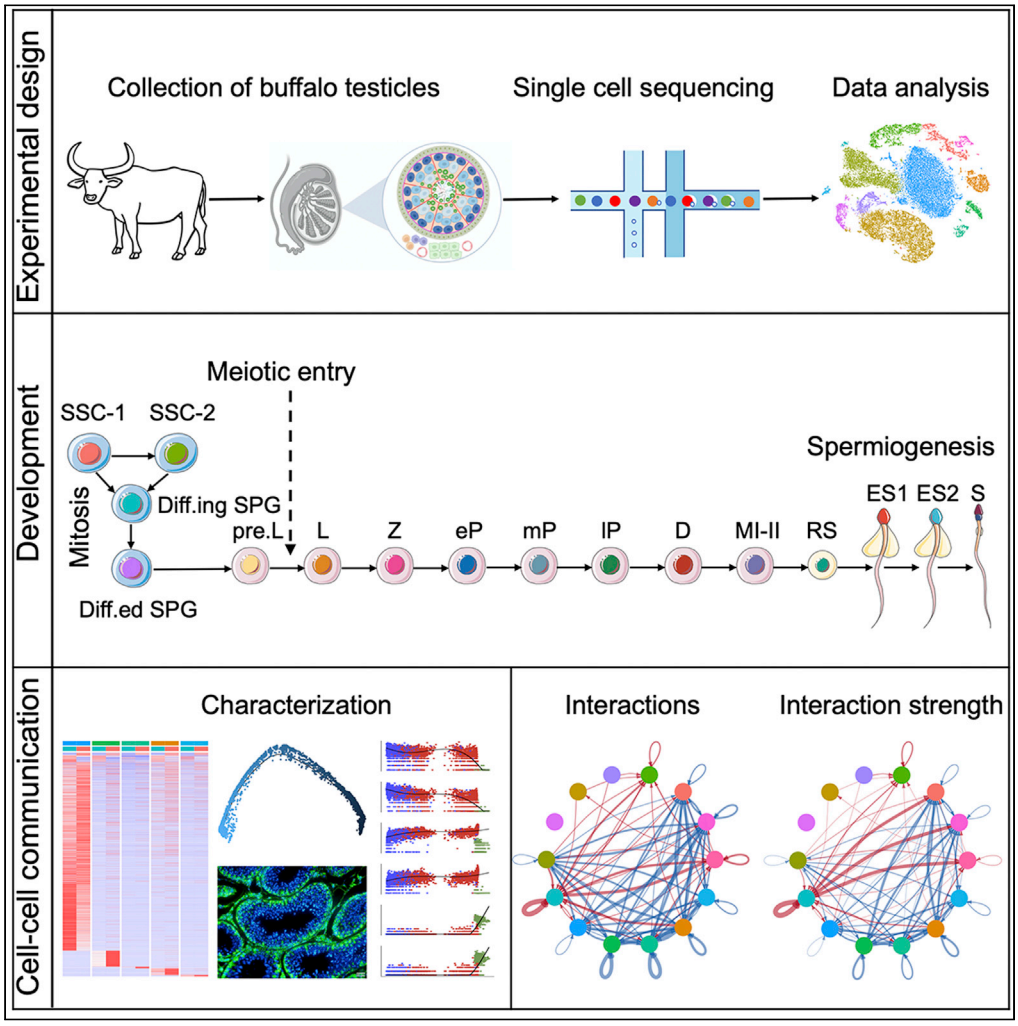

Liangfeng Huang, Junjun Zhang, Pengfei Zhang, ..., Yangqing Lu, Ming Zhang, Qiang Fu

lyq@gxu.edu.cn (Y.L.)
mingzhang@gxu.edu.cn (M.Z.)
gxfuq@gxu.edu.cn (Q.F.)

Highlights

Single-cell RNA sequencing uncovers heterogeneity of cell types in buffalo testes

Trajectory analysis reveals sequential differentiation events in germ cells

Pseudotime analysis uncovers dynamic roadmap of germ cell development

Prepubertal and pubertal buffalo testes: Comparative global cell-cell communication

Huang et al., iScience 26, 105733
January 20, 2023
https://doi.org/10.1016/j.isci.2022.105733

iScience

CellPress
OPEN ACCESS

Article

Single-cell RNA sequencing uncovers dynamic roadmap and cell-cell communication during buffalo spermatogenesis

Liangfeng Huang,[1] Junjun Zhang,[1] Pengfei Zhang,[2] Xingchen Huang,[1] Weihan Yang,[1] Runfeng Liu,[1] Qinqiang Sun,[1] Yangqing Lu,[1,*] Ming Zhang,[1,*] and Qiang Fu[1,3,*]

SUMMARY

Spermatogenesis carries the task of precise intergenerational transmission of genetic information from the paternal genome and involves complex developmental processes regulated by the testicular microenvironment. Studies performed mainly in mouse models have established the theoretical basis for spermatogenesis, yet the wide interspecies differences preclude direct translation of the findings, and farm animal studies are progressing slowly. More than 32,000 cells from prepubertal (3-month-old) and pubertal (24-month-old) buffalo testes were analyzed by using single-cell RNA sequencing (scRNA-seq), and dynamic gene expression roadmaps of germ and somatic cell development were generated. In addition to identifying the dynamic processes of sequential cell fate transitions, the global cell-cell communication essential to maintain regular spermatogenesis in the buffalo testicular microenvironment was uncovered. The findings provide the theoretical basis for establishing buffalo germline stem cells *in vitro* or culturing organoids and facilitating the expansion of superior livestock breeding.

INTRODUCTION

The water buffalo (*Bubalus bubalis*) is a valuable animal resource that significantly contributes to the agricultural economy of many developing Asian countries by providing milk, meat, and draft power.[1,2] Nevertheless, buffalo has a poor reproductive performance, and the major cause is abnormal spermatogenesis in males.[3,4] Spermatogenesis begins at puberty and depends on the maturity of the somatic microenvironment.[5] Testicular spermatogenic cell division begins at about 12 months, but the ejaculate contains a high percentage of viable spermatozoa only after 24–30 months.[6] In the testicular seminiferous tubules, some spermatogonial stem cell (SSC) populations maintain stem cell pools by self-renewal, whereas the other SSCs differentiate to form highly proliferative spermatogonia (SPG).[5,7] SPG proliferate into primary spermatocytes by mitosis, which then undergo two meiotic divisions in response to hormones such as follicle-stimulating hormone and testosterone to form haploid spermatids,[6] and subsequently spermiogenesis into spermatozoa.[8] Testicular somatic cells regulate spermatogenesis by secreting cytokines and regulating transduction of specific signals, thus controlling the balance between SSC self-renewal and differentiation, as well as secreting hormones/immunomodulatory factors, leading to an immune-privileged environment, and physical barriers.[9–14] Obviously, mammalian male pubertal development involves an increase in testicular volume, complex hormonal and molecular regulation, and cellular interactions, which ensure the success of cell proliferation, differentiation, and spermatogenesis.[5,6,15–19]

Spermatogenesis carries out the precise intergenerational transmission of paternal genetic information, representing a critical guarantee for the reproduction and continuation of the species.[20–22] Traditional bulk RNA sequencing (RNA-seq) requires total RNA collected from hundreds or thousands of cells, and the resulting expression matrix fails to distinguish among the distinct gene expression patterns from every spermatogenic cell type.[23] Purification of transient cells remains exceedingly challenging, whereas single-cell RNA-seq (scRNA-seq) technology makes it possible to visualize the status of these cells without purification and provides numerous distinctive cell stage-specific markers.[24] It helps in detecting the cell lineage and heterogeneity of all cell types in the original physiological state, revealing the different

[1]State Key Laboratory for Conservation and Utilization of Subtropical Agro-bioresources, College of Animal Science and Technology, Guangxi University, Nanning 530004, China

[2]Institute of Medical and Health, Guangxi Academy of Sciences, Nanning 530007, China

[3]Lead contact

*Correspondence: lyq@gxu.edu.cn (Y.L.), mingzhang@gxu.edu.cn (M.Z.), gxfuq@gxu.edu.cn (Q.F.)

https://doi.org/10.1016/j.isci.2022.105733

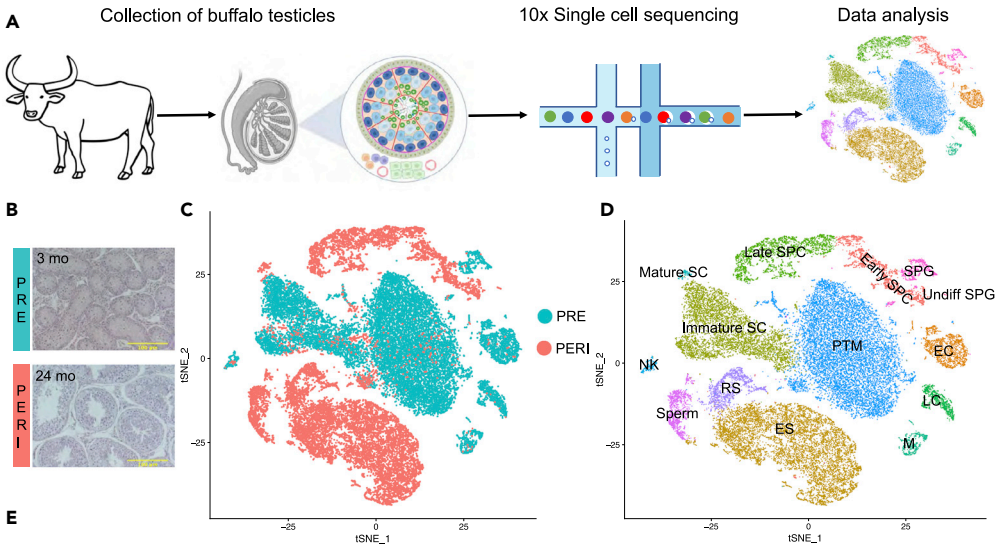

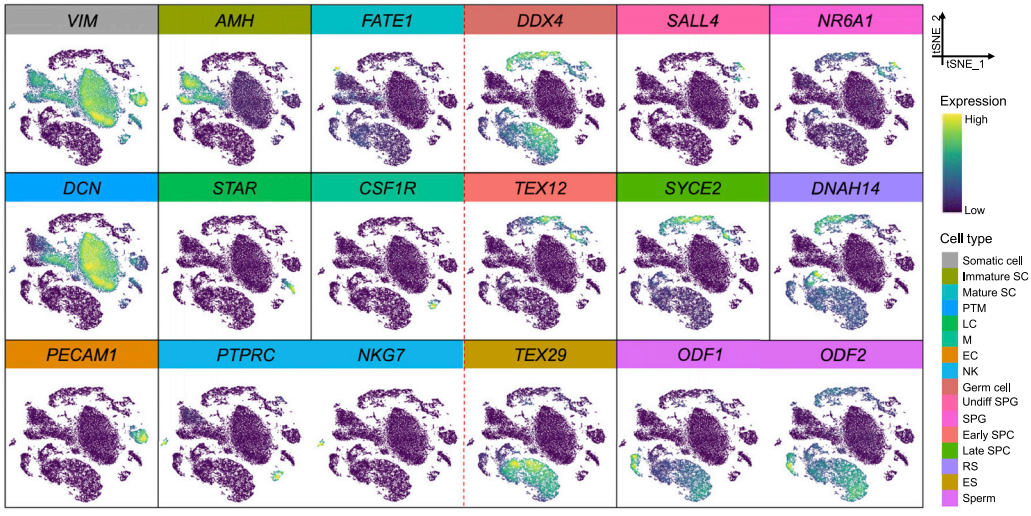

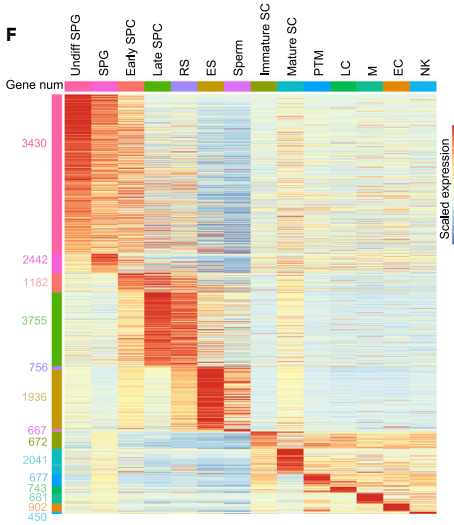

G

	Germ cell		Somatic cell
Undiff SPG	gene expression chromosome organization RNA processing	Immature SC	cotranslational protein targeting to membrane protein targeting translation
SPG	chromosome organization RNA splicing cell cycle process	Mature SC	single-organism metabolic process small molecule metabolic process cellular component organization or biogenesis
Early SPC	meiotic cell cycle process sexual reproduction DNA recombination	PTM	protein targeting to membrane muscle tissue development response to growth factor
Late SPC	cell cycle sexual reproduction gamete generation	LC	protein targeting to membrane translation steroid metabolic process
RS	sexual reproduction gamete generation reproductive process	M	immune system process response to stimulus cell activation
ES	male gamete generation germ cell development fertilization	EC	protein targeting to membrane endothelial cell migration endothelial cell proliferation
Sperm	sexual reproduction male gamete generation multicellular organism reproduction	NK	regulation of immune system process lymphocyte activation defense response

Figure 1. Single-cell transcriptome analysis of buffalo prepubertal and pubertal testes

(A) Schematic diagram of the experimental workflow.

(B) Histomorphometric analysis (H&E staining) of prepubertal and pubertal buffalo testes. Scale bar, 100 μm.

(C) Dimension reduction presentation (by tSNE) of combined single-cell transcriptome data from prepubertal and pubertal testes (a total of 32,847 cells). Each point represents a single cell and is colored by sample.

(D) tSNE plot of prepubertal and pubertal testicular cell clusters defined by scRNA-seq analysis, colored according to cell type.

(E) Expression pattern of selected markers on the tSNE plot.

(F) Heatmap of normalized expression in DEGs (Wilcoxon rank sum test, p-value < 0.05) for each cell type. Labels indicate cell type (columns) and the number of genes (rows).

(G) GO terms (biological process) for identified cell types (p-value <0.05).

molecular events of spermatogenic cell sequential occurrence and gene expression regulatory mechanisms during spermatogenesis.[25]

Recent studies have obtained stage-specific gene markers in human testicular germ cells by scRNA-seq, such as *HMGA1*, *PIWIL4*, *TEX29*, *SCML1*, and *CCDC112*.[26] At the single-cell level, several studies elucidated adult testicular germ cell–somatic cell interactions and human pubertal testicular development.[27,28] Besides, the developmental landscape of the human male germline and its somatic cells was illustrated in another single-cell study, which contributed to studies of SSC therapy.[29] In human, macaque, and mouse testes, scRNA-seq has been used to identify transcriptional signatures of major germ cells and somatic cell types, revealing spermatogonial stem/progenitor cell pools, differentiation markers, potential meiosis regulators, and germ cell–somatic cell communication mechanisms.[30] Furthermore, single-cell transcript levels of various cell types during spermatogenesis in sheep and pigs have been demonstrated.[31,32] Hence, the development patterns and gene expression of spermatogenic cells during spermatogenesis have both similarities and differences among species.[33]

Nevertheless, mammalian spermatogenesis is mostly understood from studies on rodents, monkeys, and humans.[13,25,27,28,34–39] Conversely, significant differences exist among species in the seminiferous epithelial cycle, spermatogenesis cycle, the developmental pattern of SPG, specific molecular markers, etc.[17,40–43] These differences between species make it difficult to establish germline stem cells or perform organoid culture *in vitro*, which prevents us from understanding the biological functions of germline stem cells, the complexity of spermatogenesis, and the regulation of the male germline.[44] Similarly, it also hinders investigation into the expansion of superior livestock breeding and the establishment of livestock models.[45–47] In the present study, single-cell RNA-seq data was obtained from prepubertal (PRE, 3-month-old) and pubertal (PERI, 24-month-old) buffalo testes. Spermatogenic and somatic cell clusters were identified; a high precision single-cell transcriptional atlas of spermatogenesis and somatic cell development was generated; and the similarities and differences in cell-cell communication networks between prepubertal and pubertal testes and stage-specific markers were elucidated. Our work reveals single-cell gene expression patterns in prepubertal and pubertal buffalo testes, providing crucial insights into the molecular mechanisms that underpin spermatogenesis and germ cell development. Furthermore, it presents a molecular theoretical foundation for investigating mechanisms in stem cell maintenance and organoid culture.

RESULTS

Single-cell transcriptome of buffalo prepubertal and pubertal testes

To characterize the cell types of buffalo testes, cells were isolated from 3-month-old (prepuberty) and 24-month-old (puberty) healthy buffalo testicular samples and obtained a total of 32,847 cells (after quality control filtration) were obtained by 10x single-cell sequencing (Figures 1A, S1A, and S1B). Furthermore, after morphological analysis (hematoxylin and eosin staining) of buffalo prepubertal and pubertal testes, it was observed that the prepubertal testis lacked a tubular lumen, whereas the pubertal testis already developed a complete tubular lumen with germ and somatic cells at all stages, and spermatogenesis was complete (Figure 1B). Subsequently, the t-distributed stochastic neighbor embedding (tSNE) analysis was performed on all sample sequencing data using the Seurat package in R, resulting in a total of 14 major clusters, which were subsequently annotated using identified genetic markers (Figures 1C and 1D).

The cell types and markers are as follows: Immature Sertoli cell (Immature SC, *AMH*$^+$/*INHA*$^+$/*CLU*$^+$), mature Sertoli cell (Mature SC, *FATE1*$^+$/*HMGN5*$^+$/*CLDN11*$^+$), peritubular myoid cell (PTM, *DCN*$^+$/*PDGFRA*$^+$/*PTCH1*$^+$), Leydig cell (LC, *STAR*$^+$/*HSD3B1*$^+$/*INSL3*$^+$), macrophage (M, *CSF1R*$^+$/*CD74*$^+$/*MAFB*$^+$), endothelial

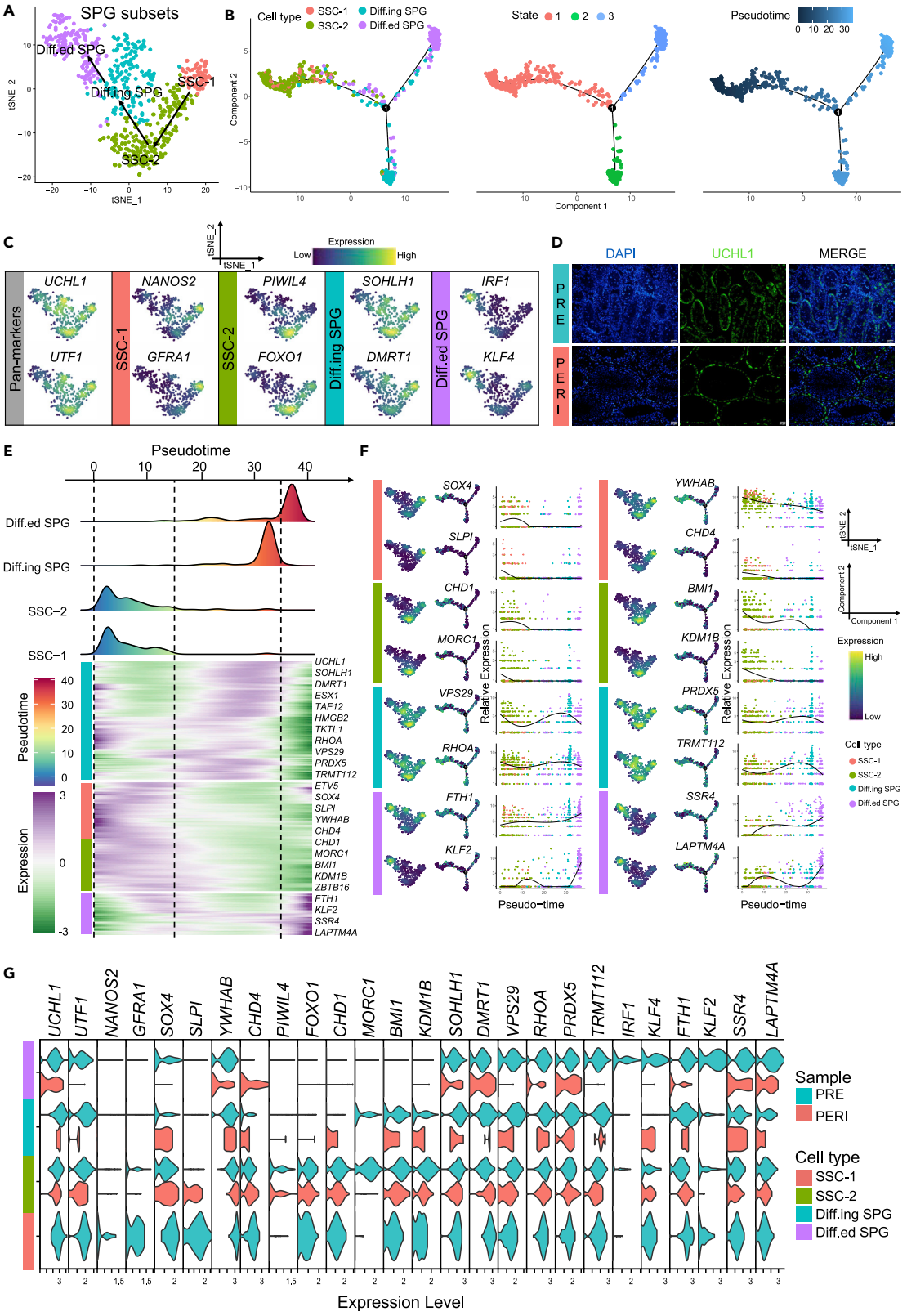
A
SPG subsets
Diff.ed SPG
Diff.ing SPG
SSC-1
SSC-2
tSNE_1
tSNE_2
B
Cell type
SSC-1
SSC-2
Diff.ing SPG
Diff.ed SPG
State
Pseudotime
Component 1
Component 2
C
Expression
Low
High
Pan-markers
UCHL1
UTF1
SSC-1
NANOS2
GFRA1
SSC-2
PIWIL4
FOXO1
Diff.ing SPG
SOHLH1
DMRT1
Diff.ed SPG
IRF1
KLF4
D
DAPI
UCHL1
MERGE
PRE
PERI
E
Pseudotime
Diff.ed SPG
Diff.ing SPG
SSC-2
SSC-1
Pseudotime
Expression
UCHL1
SOHLH1
DMRT1
ESX1
TAF12
HMGB2
TKTL1
RHOA
VPS29
PRDX5
TRMT112
ETV5
SOX4
SLPI
YWHAB
CHD4
CHD1
MORC1
BMI1
KDM1B
ZBTB16
FTH1
KLF2
SSR4
LAPTM4A
F
SOX4
SLPI
CHD1
MORC1
VPS29
RHOA
FTH1
KLF2
YWHAB
CHD4
BMI1
KDM1B
PRDX5
TRMT112
SSR4
LAPTM4A
Relative Expression
Pseudo−time
Expression
High
Low
Cell type
SSC-1
SSC-2
Diff.ing SPG
Diff.ed SPG
G
UCHL1
UTF1
NANOS2
GFRA1
SOX4
SLPI
YWHAB
CHD4
PIWIL4
FOXO1
CHD1
MORC1
BMI1
KDM1B
SOHLH1
DMRT1
VPS29
RHOA
PRDX5
TRMT112
IRF1
KLF4
FTH1
KLF2
SSR4
LAPTM4A
Sample
PRE
PERI
Cell type
SSC-1
SSC-2
Diff.ing SPG
Diff.ed SPG
Expression Level

Figure 2. Identification of SPG subsets in prepubertal and pubertal buffalo

(A) Re-clustering tSNE plot of SPG subsets in buffalo testes.

(B) Pseudotime trajectories of buffalo SPG subsets, colored by cell type, state, and pseudotime value.

(C) Feature plots of marker genes for SSC-1, SSC-2, Diff.ing SPG, and Diff.ed SPG.

(D) IF analysis of antibody staining against UCHL1 on paraffin sections of prepubertal and pubertal buffalo testes. Scale bar, 20 μm.

(E) Heatmap of DEGs (q-value < 0.01) expression (rows) along the pseudotime (columns). The heatmap shows cell types (left) and the representative genes (right) for each cell type.

(F) Feature plots, trajectory plots, and pseudotime trajectory expression patterns of selected marker genes in SSC-1, SSC-2, Diff.ing SPG, and Diff.ed SPG.

(G) Violin plot of the selected gene expression split by sample.

cell (EC, *PECAM1*$^+$/*CLDN5*$^+$/*ECSCR*$^+$), natural killer cell (NK, *PTPRC*$^+$/*NKG7*$^+$/*KLRF1*$^+$/*CD94*$^+$), undifferentiated spermatogonia (Undiff SPG, *SALL4*$^+$/*ZBTB16*$^+$/*ELAVL2*$^+$), spermatogonia (SPG, *NR6A1*$^+$/*FGFR3*$^+$/*FMR1*$^+$), early-stage primary spermatocyte (from preleptotene to zygotene) (Early SPC, *TEX12*$^+$/*SMCHD1*$^+$/*PRSS50*$^+$), late-stage spermatocyte (from pachytene to secondary spermatocyte) (Late SPC, *SYCE2*$^+$/*BOLL*$^+$/*MLH1*$^+$), round spermatid (RS, *DNAH14*$^+$/*IZUMO4*$^+$/*NKAPL*$^+$), elongating/elongated spermatid (ES, *TEX29*$^+$/*FBXO24*$^+$/*ACRV1*$^+$), and spermatozoa (Sperm, *ODF1*$^+$/*ODF2*$^+$/*OAZ3*$^+$/*AKAP4*$^+$) (Figures 1E, S1C, and S1D).

In the germ cell cluster (*DDX4*$^+$), 3430, 2442, 1182, 3755, 756, 1936, and 667 differentially expressed genes (DEGs) were obtained for Undiff SPG, SPG, Early SPC, Late SPC, RS, ES, and Sperm, respectively; whereas in the somatic cell cluster (*VIM*$^+$), Immature SC, Mature SC, PTM, LC, M, EC, and NK cells had 672, 2041, 677, 743, 681, 902, and 450 DEGs, respectively (Figure 1F and Table S1). Gene ontology (GO) terms for each cell type supported the definition. For instance, clusters in germ cell development contained "chromosome organization", "sexual reproduction", and "male gamete generation". Also, somatic cells reflected the GO terms for functional characteristics in the physiological state (Figure 1G and Table S2).

Trajectory analysis of spermatogonial cells

Spermatogonial mitosis is the first step to mammalian spermatogenesis.[48] The original clustering analysis (Figure 1D) showed that spermatogonia consisted of two cell clusters (Undiff SPG and SPG, 626 cells). To further characterize the cellular subtypes and transitional relationships of spermatogonia from prepubertal and pubertal buffalo testes, Undiff SPG and SPG clusters were re-clustered to obtained SSC-1, SSC-2, Diff.-ing SPG (differentiating) and Diff.ed SPG (differentiated) clusters (Figures 2A and S2A). A total of 1516, 1553, 510, and 310 DEGs with elevated expression at different developmental stages were determined by the Seurat package (Figure S2B and Table S3). Subsequently, cell trajectory analysis of the four cell types was performed using the Monocle package, and the pseudotime value confirmed the differentiation relationship of the re-clustered cells (Figure 2B).

The SPG subsets all broadly expressed *UCHL1* and *UTF1* (SPG pan-marker).[28,49] Many previously identified and new SSC marker genes were expressed by SSC-1 and SSC-2, including *DAZL*,[50] male germline stem cell asymmetric division-related genes (e.g., *ZBTB16*, *ELAVL2*, and *HUWE1*). *ITGA6*, *ETV4*, *ETV5*, and *ST3GAL2* showed high expression levels in SSC-1 (*NANOS2*$^+$/*GFRA1*$^+$). In SSC-2 (*PIWIL4*$^+$/*FOXO1*$^+$), *RBM47*, *PRC1*, *HELLS*, and *CXADR* were exceedingly expressed. Furthermore, Diff.ing SPG (*SOHLH1*$^+$/*DMRT1*$^+$) strikingly expressed genes promoting spermatogonial differentiation (*ESX1*, *CCDC124*, *TMEM147*, and *NDUFA4*). Finally, Diff.ed SPG specifically expressed the spermatogonial promitogenic factor (*IRF1*),[51] pluripotency transcription factors (TFs) (*KLF4*),[52,53] *CLEC3B*, *DBI*, *PPIB*, and *IER2* (Figures 2C and S2C). As expected, immunofluorescence (IF) staining found that UCHL1 was located on the basal membrane of testicular seminiferous tubules in both PRE and PERI, consistent with the location of spermatogonial distribution, demonstrating that it could function as a pan-marker for every stage of SPG in buffalo (Figure 2D).

Monocle-derived pseudotime analysis showed dynamic expression patterns of multiple genes along the SPG differentiation timeline (Figure 2E). In addition, *SOX4* was highly expressed in SSC-1, whereas *SLPI*, *YWHAB*, *CHD4*, *HMGA1*, *RRBP1*, *ZNF518A*, and *RAC1* showed expression trends in the pseudotime axis consistent with the tSNE re-clustering results. *CHD1* was specifically expressed in SSC-2, and we also found that *MORC1*, *BMI1*, *KDM1B*, *ITGB1*, *LPIN2*, *GTF2A1*, and *RBBP8* shared the same expression pattern.

Besides, *VPS29*, *RHOA*, *PRDX5*, *TRMT112*, *ATP5F1E*, *EIF1AX*, *NDUFV2*, and *PSMG4* showed a similar pattern to markers *SOHLH1*, *ESX1*, and *DMRT1*, which are known to be present in differentiating spermatogonia. Several pluripotency markers (*KLF2* and *KLF4*), *FTH1*, *SSR4*, *LAPTM4A*, *HSPB1*, *ANXA1*, *SELENOM*,

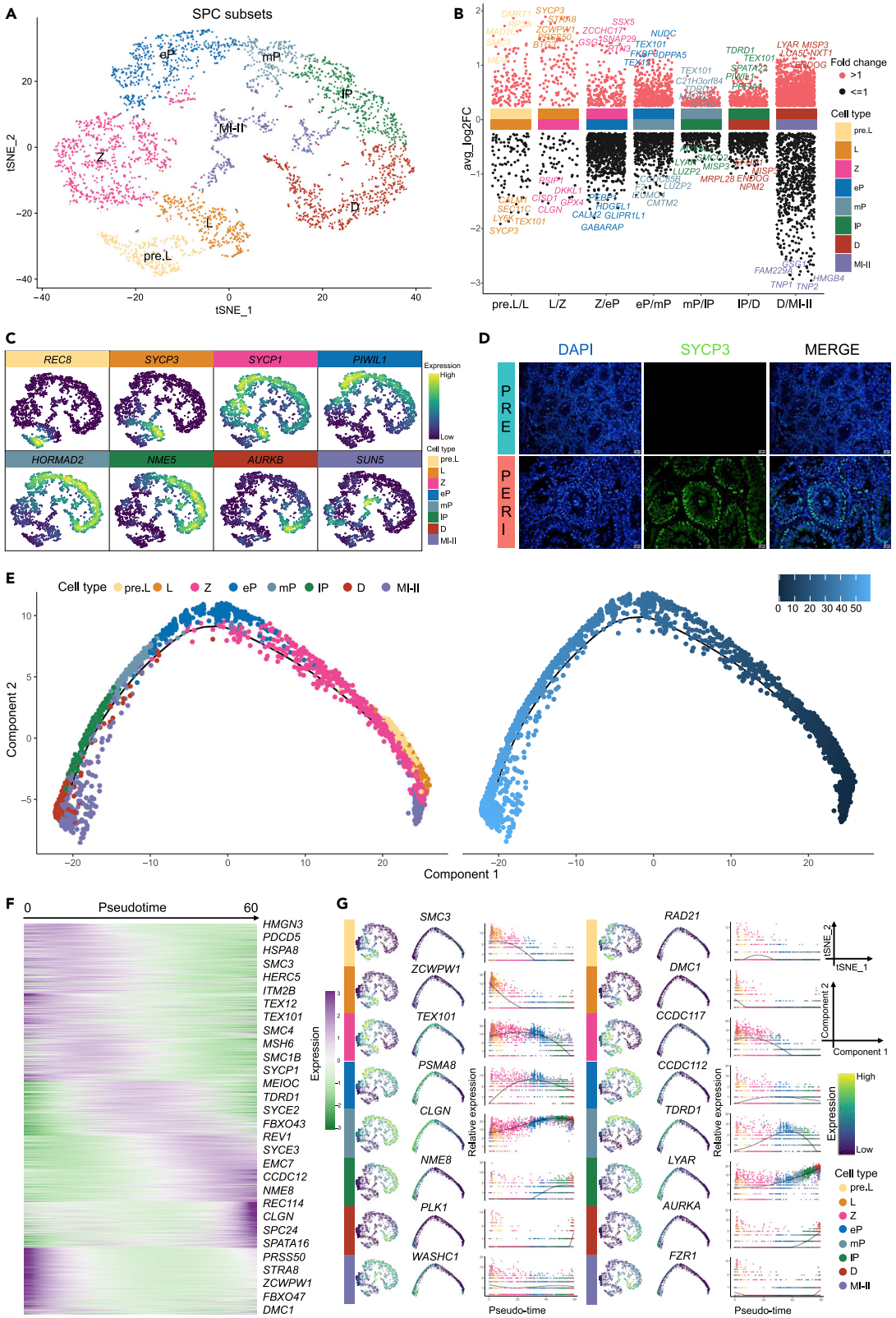
A
SPC subsets
eP
mP
IP
MI-II
Z
D
L
pre.L
tSNE_2
tSNE_1
B
avg_log2FC
Fold change
>1
<=1
Cell type
pre.L
L
Z
eP
mP
IP
D
MI-II
pre.L/L
L/Z
Z/eP
eP/mP
mP/IP
IP/D
D/MI-II
C
REC8
SYCP3
SYCP1
PIWIL1
HORMAD2
NME5
AURKB
SUN5
Expression
High
Low
Cell type
D
DAPI
SYCP3
MERGE
PRE
PERI
E
Cell type
pre.L
L
Z
eP
mP
IP
D
MI-II
0 10 20 30 40 50
Component 2
Component 1
F
0
Pseudotime
60
HMGN3
PDCD5
HSPA8
SMC3
HERC5
ITM2B
TEX12
TEX101
SMC4
MSH6
SMC1B
SYCP1
MEIOC
TDRD1
SYCE2
FBXO43
REV1
SYCE3
EMC7
CCDC12
NME8
REC114
CLGN
SPC24
SPATA16
PRSS50
STRA8
ZCWPW1
FBXO47
DMC1
Expression
G
SMC3
ZCWPW1
TEX101
PSMA8
CLGN
NME8
PLK1
WASHC1
RAD21
DMC1
CCDC117
CCDC112
TDRD1
LYAR
AURKA
FZR1
Relative expression
Pseudo-time
tSNE_2
tSNE_1
Component 2
Component 1
Expression
High
Low
Cell type
pre.L
L
Z
eP
mP
IP
D
MI-II

Figure 3. Identification of SPC subsets in buffalo

(A) Re-clustering tSNE plot of SPC subsets in buffalo testes.

(B) Multi-volcano plot showing meiotic genes (test.use = "wilcox", min.pct = 0.65) in pairwise comparisons in all cell types. The graph displayed the top five annotated genes with the most fold change for each group.

(C) Feature plots of representative marker genes for pre.L, L, Z, eP, mP, lP, D, and MI-II.

(D) IF analysis of antibody staining against SYCP3 on paraffin sections of prepubertal and pubertal buffalo testes. Scale bar, 20 μm.

(E) Pseudotime trajectories of buffalo SPC subsets, colored by cell type (left) and pseudotime value (right).

(F) Heatmap showing DEGs (q-value < 0.01) expression (rows) along the pseudotime (columns) axis.

(G) Feature plots, trajectory plots, and pseudotime trajectory expression patterns of selected genes in pre.L, L, Z, eP, mP, lP, D, and MI-II.

and *FAU* showed similar pseudotime expression patterns and were highly expressed in Diff.ed SPG (Figures 2F and S2D). Thus, the data revealed the dynamic expression pattern of SPG subsets along the developmental pseudotime trajectory, and these stage-specific markers could be used to construct regulatory networks of male germ cells in breeding livestock.

To further elucidate the heterogeneity of prepubertal and pubertal buffalo spermatogonial differentiation, the expression of spermatogonial stage markers was split by sample (PERI vs. PRE). Importantly, *NANOS2*, *GFRA1*, *ST3GAL2*, and *MORC1* were only found to be specifically expressed in PRE-derived SSC, whereas *IRF1*, *KLF2*, and *KLF4* were only found in PRE-derived Diff.ed SPG. All phases of PRE- and PERI-derived SPG subsets were identified by the remaining candidate markers (Figures 2G and S2E).

Identification of spermatocytes in buffalo

The second step of mammalian spermatogenesis is spermatocyte meiosis.[54] SPC subsets (Early SPC and Late SPC, 3,782 cells) were re-clustered into cell populations, yielding eight clusters of spermatocytes at distinct developmental phases, namely, pre.L (preleptotene), L (leptotene), Z (zygotene), eP (early pachytene), mP (middle pachytene), lP (late pachytene), D (diplotene), and MI-II (mixed cells of primary and secondary spermatocytes) (Figures 3A and S3A, and Table S3). Next, meiosis-associated genes were calculated by the FindMarkers function of Seurat package for actively high-variable genes across sequential spermatocyte stages during meiosis (Figure 3B and Table S4). Meiosis-associated genes were linked to the following spermatocyte stages: DNA synthesis, sister chromatid cohesion, axial elements, homologous chromosome pairing, DNA double-strand break (DSB) formation, synaptonemal complex formation, recombination, nuclear envelope breakdown, and a series of molecular events during spermatogenesis from pre-meiosis to meiosis.[55–60]

The meiosis-associated genes *REC8*, *SMC3*, and *DMRTB1*[35,57,61] were found to be specifically expressed in pre.L spermatocytes. Further, the meiosis initiation marker *STRA8*, synaptonemal complex protein 3 (*SYCP3*), homologous chromosome pairing-related genes at meiosis (*ZCWPW1*), and DNA meiotic recombinase 1 (*DMC1*)[62–64] tended to be highly expressed in L spermatocytes. In Z spermatocytes, the meiosis-specific genes *SYCP1*, *TEX101*, and *MEIOB*[65] were acutely expressed. Moreover, the piwi family members *PIWIL1* and *CCDC112*[26,37] are biomarkers for the beginning of expression in eP spermatocytes. In mP spermatocytes, the central element deposition-related marker *HORMAD2* and the pseudoautosomal region-related marker *REC114*[66–68] were substantially expressed. In lP spermatocytes, the tubulin-binding and microtubule motor activity-related genes *NME5* and *NME8*[26,32,65] were expressed. The D spermatocytes express aurora kinase A/B (*AURKA* and *AURKB*).[25,26] Finally, meiotic nuclear division-related genes *SUN5*, *SUN3*, and *FZR1*[26,38,64,65] were expressed in MI-II spermatocytes (Figures 3C, S3B, and S3C). Actually, IF staining showed that the distribution of leptotene spermatocytes corresponded to the localization of SYCP3 in buffalo testes from PRE and PERI (Figure 3D).

The classification of cells at each stage of SPC subsets was confirmed by pseudotime trajectory analysis of buffalo spermatocytes (Figure 3E). To better understand the sequential gene expression patterns during meiosis, spermatocyte-specific marker gene expression at every stage was matched to cell developmental trajectories (Figure 3F). In pre-meiotic spermatocytes (pre. L), *RAD21* (nuclear meiotic cohesin complex), *SMC1A* (meiotic cell cycle gene), *SMC3* (cohesin complex), *DMRTB1*(coordinate the developmental transition from spermatogonial differentiation to meiotic entry), *HMGN3* (the chromatin-binding protein), and *MIF* (glycosylation-inhibiting factor) were specifically expressed, which decreases as pseudotime development increases, and essentially no expression occurs after Z spermatocytes. In L spermatocytes, *ZCWPW1*, *DMC1*, *STRA8*, *PRSS50*, *RAD21L1*, and *BTG3* were strongly expressed, whereas following Z spermatocytes, their expression was almost absent. *TEX101*, *CCDC117*,

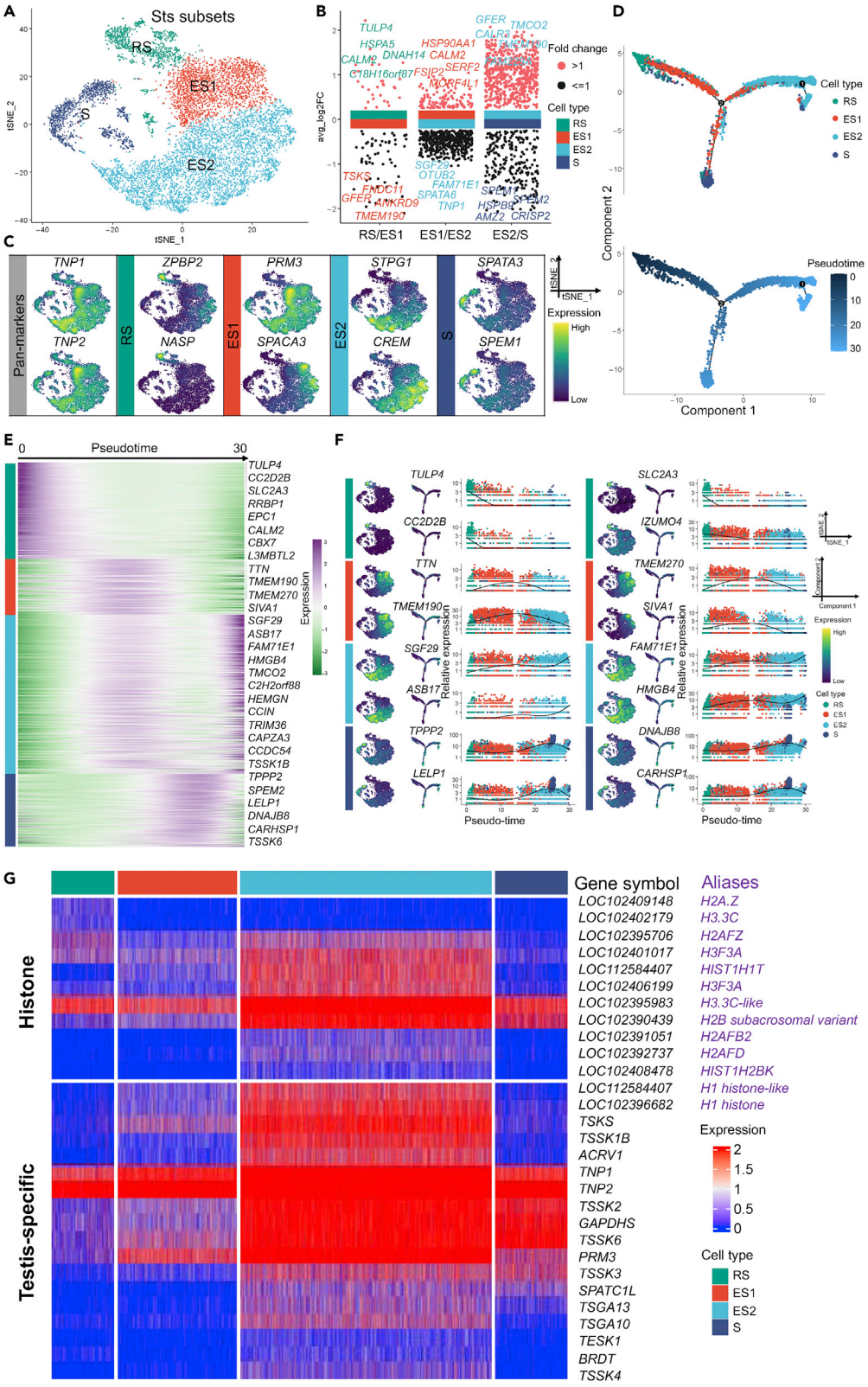
A
Sts subsets
RS
ES1
S
ES2
tSNE_1
tSNE_2
B
avg_log2FC
Fold change
>1
<=1
Cell type
RS
ES1
ES2
S
RS/ES1
ES1/ES2
ES2/S
C
Pan-markers
RS
ES1
ES2
S
TNP1
TNP2
ZPBP2
NASP
PRM3
SPACA3
STPG1
CREM
SPATA3
SPEM1
Expression
High
Low
D
Cell type
Component 1
Component 2
Pseudotime
E
Pseudotime
Expression
F
Relative expression
Pseudo-time
G
Histone
Testis-specific
Gene symbol
Aliases
LOC102409148 H2A.Z
LOC102402179 H3.3C
LOC102395706 H2AFZ
LOC102401017 H3F3A
LOC112584407 HIST1H1T
LOC102406199 H3F3A
LOC102395983 H3.3C-like
LOC102390439 H2B subacrosomal variant
LOC102391051 H2AFB2
LOC102392737 H2AFD
LOC102408478 HIST1H2BK
LOC112584407 H1 histone-like
LOC102396682 H1 histone
TSKS
TSSK1B
ACRV1
TNP1
TNP2
TSSK2
GAPDHS
TSSK6
PRM3
TSSK3
SPATC1L
TSGA13
TSGA10
TESK1
BRDT
TSSK4
Expression
Cell type
RS
ES1
ES2
S

Figure 4. Identification of Sts subsets in buffalo

(A) Re-clustering tSNE plot of Sts subsets in buffalo testes.

(B) Multi-volcano plot showing spermiogenesis-related genes (test.use = "wilcox", min.pct = 0.65) in pairwise comparisons in all cell types (RS, ES1, ES2, and S).

(C) Feature plots of representative marker genes for RS, ES1, ES2, and S.

(D) Pseudotime trajectories of buffalo Sts subsets, colored by cell type (up) and pseudotime value (down), respectively.

(E) Heatmap showing DEGs (q-value < 0.01) expression (rows) along the pseudotime (columns) axis.

(F) Feature plots, trajectory plots, and pseudotime trajectory expression patterns of selected genes in RS, ES1, ES2, and S.

(G) Heatmap of histone and testis-specific gene expression in RS, ES1, ES2, and S.

SETX, *TOP2B*, *WDR82*, and *C11H14orf39* were highly expressed in Z and underexpressed in eP spermatocytes.

Synaptonemal complex protein 2 (*SYCP2*), meiotic spindle-related genes (*HSPA2*, *SELENOW*, and *PEBP1*), and meiotic cell cycle-related gene (*PSMA8*) showed the highest expression in eP spermatocytes and gradually decreased with the increase in pseudotime. Meiotic cell cycle-related genes (*CLGN* and *TDRD1*), meiotic recombination protein (*REC114*), *GPATCH4*, *SAMD15*, and *MRPS26* were continually expressed with the pseudo-development axis, whereas *CLGN* and *TDRD1* expression in the pre.L–mP spermatocyte stage progressively increased and the expression of mP–D spermatocyte stage gradually decreased.

Furthermore, *NME8* and cell growth-regulating nucleolar protein (*LYAR*, *ADAM2*, *MLLT10*, *CCDC38*, and *CCDC85B*) were continuously expressed in the lP–D spermatocyte stage, with the maximum expression in lP. Then, *PLK1* (meiotic cytokinesis), *AURKA* (meiotic spindle), *MISP3*, *NPM2* (positive regulation of meiotic nuclear division), *INCENP* (meiotic spindle midzone assembly), and *CCNA1* (meiotic cell cycle) began to be expressed in lP and peaked in the D spermatocyte stage. Ultimately, *WASHC1* (meiotic spindle assembly), *FZR1* (regulation of meiotic nuclear division), *CCER1*, *CLDND2*, *FBXO39* (F-box protein family member), and *TMEM89* were specifically expressed only in MI-II spermatocytes (Figures 3G and S3D). In summary, the data presented candidate-specific gene markers for the above stages of spermatocytes.

Dynamic gene expression patterns during spermiogenesis

Spermiogenesis is the final stage of spermatogenesis.[8,69] Original RS, ES, and Sperm clusters (Sts subsets, 9,629 cells) were re-clustered into four haploid spermatids—RS (round spermatid), ES1 (elongating spermatid), ES2 (elongated spermatid), and S (spermatozoa) (Figures 4A, S4A, and S4B, and Table S3). To obtain highly variable genes that are active during spermiogenesis, spermiogenesis-related genes were calculated by the FindMarkers function of the Seurat package (Figure 4B and Table S4). The spermatid pan-marker transition protein (*TNP1* and *TNP2*)[70] is expressed in RS, ES1, ES2, and S. Initially, RS was identified by the zona pellucida binding protein 2 (*ZPBP2*) and nuclear autoantigenic sperm protein (*NASP*).[27,71] For ES1, protamine 3 (*PRM3*) and sperm acrosome-associated 3 (*SPACA3*)[27,72] were marked. Next, ES2 was marked by sperm tail PG-rich repeat containing 1 (*STPG1*) and cAMP response element modulator (*CREM*).[73] Finally, S was characterized by spermatogenesis-associated 3 (*SPATA3*) and spermatid maturation 1 (*SPEM1*)[74–76] (Figure 4C).

The analysis of pseudotime trajectories provided evidence to support the categorization of spermatid development (Figure 4D), and the identification of expression patterns of multiple genes related to spermatid differentiation, resulting in distinct genetic markers for individual spermatid stages (Figure 4E). For instance, the expression of *TULP4*, *CC2D2B*, *SLC2A3*, *IZUMO4*, *SPATA22*, and *STRBP* was specifically detected at the RS stage, with decreasing expression levels as pseudotime increased. Specifically, *TTN*, *TMEM190*, *TMEM270*, *SIVA1*, *SPACA1*, and *TEX29* were considered candidate genes for ES1-specific expression. Genes related to spermatid development (*SGF29*, *ASB17*, *FAM71E1*, and *HMGB4*) and sperm tail development-related genes (*MEIG1* and *KLC3*)[77] were categorized into candidate genes for ES2. Finally, *TPPP2*, *LELP1*, *DNAJB8*, *CARHSP1*, *AKAP4*, and *SPACA9* were recognized as candidate markers for the S cluster (Figures 4F, S4C, and S4D).

Histone-to-protamine transition is a central molecular event during spermiogenesis.[78] Consequently, the patterns of histone variants and testis-specific genes during spermiogenesis were examined, and these expressions were the strongest in ES2, demonstrating that transcriptional activity peaking during ES2 was associated with a histone-to-protamine transition (Figures 4G and S4E).

A

SSC-1 ~chromatin organization ~positive regulation of transcription from RNA polymerase II promoter ~negative regulation of transcription from RNA polymerase II promoter ~mRNA processing ~regulation of transcription, DNA-templated	SSC-2 ~ubiquitin-dependent protein catabolic process ~positive regulation of transcription from RNA polymerase II promoter ~chromatin organization ~peptidyl-serine phosphorylation ~protein deubiquitination	Diff.ing SPG ~mitochondrial respiratory chain complex I assembly ~protein folding ~mitochondrial electron transport, NADH to ubiquinone ~mRNA splicing, via spliceosome ~translation	Diff.ed SPG ~translation ~cytoplasmic translation ~extracellular matrix organization ~transforming growth factor beta receptor signaling pathway ~modification-dependent protein catabolic process
eP ~translation ~mitochondrial respiratory chain complex I assembly ~mRNA splicing, via spliceosome ~cytoplasmic translation ~piRNA metabolic process	Z ~mRNA splicing, via spliceosome ~mRNA processing ~RNA splicing ~spermatogenesis ~ubiquitin-dependent protein catabolic process	L ~protein folding ~mRNA splicing, via spliceosome ~protein stabilization ~sister chromatid cohesion ~cell division	pre.L ~mRNA splicing, via spliceosome ~chromatin organization ~protein folding ~translation ~mRNA processing
mP ~translation ~cytoplasmic translation ~formation of cytoplasmic translation initiation complex ~mitochondrial respiratory chain complex I assembly ~mitochondrial ATP synthesis coupled proton transport	IP ~translation ~cell division ~flagellated sperm motility ~cilium assembly ~binding of sperm to zona pellucida	D ~cell division ~cell cycle ~cilium assembly ~anaphase-promoting complex-dependent catabolic process ~proteasome-mediated ubiquitin-dependent protein catabolic process	MI-II ~spermatogenesis ~spermatid development ~flagellated sperm motility ~fusion of sperm to egg plasma membrane ~fertilization
S ~glycolytic process ~spermatogenesis ~peptidyl-serine phosphorylation ~ubiquitin-dependent protein catabolic process ~protein stabilization	ES2 ~spermatogenesis ~spermatid development ~flagellated sperm motility ~fertilization ~multicellular organism development	ES1 ~protein folding ~mitochondrial respiratory chain complex I assembly ~protein transport ~spermatogenesis ~binding of sperm to zona pellucida	RS ~protein folding ~translation ~microtubule-based movement ~mRNA processing ~RNA splicing

B

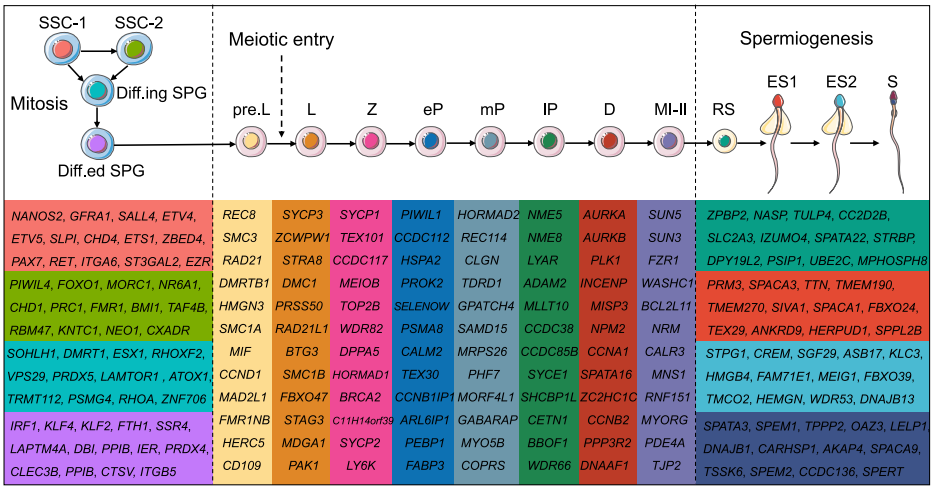

C

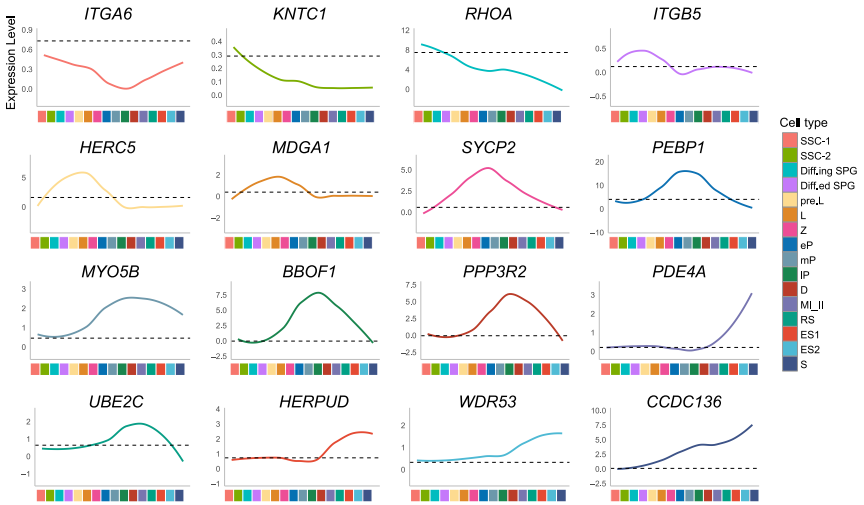

Figure 5. Transcriptome functional characteristics and sequential expression patterns of buffalo male germ cells

(A) Top five most significant GO terms (p-value < 0.05) of spermatogenic cells (by DAVID), colored by cell type.

(B) Development stage-specific gene expression patterns in buffalo spermatogenic cells, with each color palette, and nucleus color-coordinated with cell type.

(C) Cell-surface specific marker gene expression levels of spermatogenic cells.

Spermatogenic cell lineage development in buffalo

To further characterize the dynamic transcriptome on the developmental trajectory of buffalo male germ cells, the expression patterns of 16 germ cell clusters (14,037 cells) with elevated DEGs (15,097 genes) were analyzed (Figure S5A). GO analysis demonstrated that individual germ cells undergo different biological processes (Figure 5A and Table S5). These activities were consistent with the sequential molecular events involved in mammalian spermatogenic cells.[8,18,20,79]

During spermatogonial differentiation, SSC-1 and SSC-2 were mainly enriched in chromatin organization and transcription-related activities. Diff.ing SPG was coupled with activities such as mitochondrial energy, mRNA splicing, and translation, whereas Diff.ed SPG was enriched in translation and the transforming growth factor beta receptor signaling pathway.

The processes of sister chromatid cohesion and spermatogenesis were particularly enriched in early primary spermatocytes (pre.L–Z). Late primary spermatocytes (eP–D) were involved in translation, ATP synthesis-related, cell division, and cilium assembly processes, revealing that transition from meiosis to spermiogenesis was a sequential step, with genes involved in sperm structural assembly already being expressed in the lP–D spermatocytes stage. Consistent with the results of the pseudotime analysis of spermatocytes, MI-II was enriched in spermatogenesis, spermatid development, flagellated sperm motility, fusion of sperm to egg plasma membrane and fertilization, showing evidence that MI-II not only significantly expressed genes related to the breakdown of the nuclear envelope but also participated in the molecular events of early and late meiosis.

During spermiogenesis, in addition to mRNA and protein activities, RS was responsible for microtubule-based movement and other biological processes closely related to spermatid development. ES1 and ES2 were predominantly involved in spermatogenesis, spermatid development, and fertilization. Except for enrichment to spermatogenesis, S was also broadly associated with protein catabolic process and sperm motility. The GO enrichment analysis showed that several biological processes were active or cell-type-specific in the buffalo male germline cell.

Moreover, the markers with stage-specific/pseudotime-sequential expression of individual germ cell clusters were summarized in the present study (Figure 5B). To investigate cell-surface specific marker genes contributing to the cultivation of buffalo primary spermatogenic cells *in vitro*, the linear expression relationship of markers along the differentiation timeline was observed by prediction of membrane protein (Figures 5C and S5B, and Table S6).

Characterization of the somatic lineages in buffalo testes

Testicular cell-cell interactions are required for complete spermatogenesis.[16,80] Somatic cell subsets (Figures 1D, 18,810 cells) were investigated individually to characterize the gene expression patterns that establish the spermatogenic microenvironment during prepuberty and puberty (Figure 6A).

SCs are the only somatic cells in seminiferous tubules that directly interact with germ cells to regulate spermatogenesis.[9] To reveal SC differentiation, the SCs subsets (Immature and Mature SC, 5,219 cells) were re-clustered into two Immature SC clusters (Immature 1 and Immature 2) and one Mature SC cluster (Mature) (Figures 6B and S6A and Table S3). Immature 1 (*AMH*$^{+}$/*SOX9*$^{-}$), Immature 2 (*AMH*$^{+}$/*SOX9*$^{+}$), and Mature SC (*SOX9*$^{+}$/*AMH*$^{-}$) were marked by *LGALS1* and *MMP2*,[81,82] *GATA4* and *TIMP2*,[39,83] *WT1* and *CLDN11*,[84–86] respectively (Figure S6B). Strikingly, Immature 2 and Mature clusters were positive for *SOX9*, and IF staining showed that SOX9 was partially expressed in cells near the basement membrane of prepubertal and pubertal testes (Figure S6C).

Likewise, the pseudotime trajectory analysis proved that Immature 1 developed before Immature 2, which gradually differentiated into Mature SC (Figure 6C). In the dynamic gene expression pattern of SCs on the

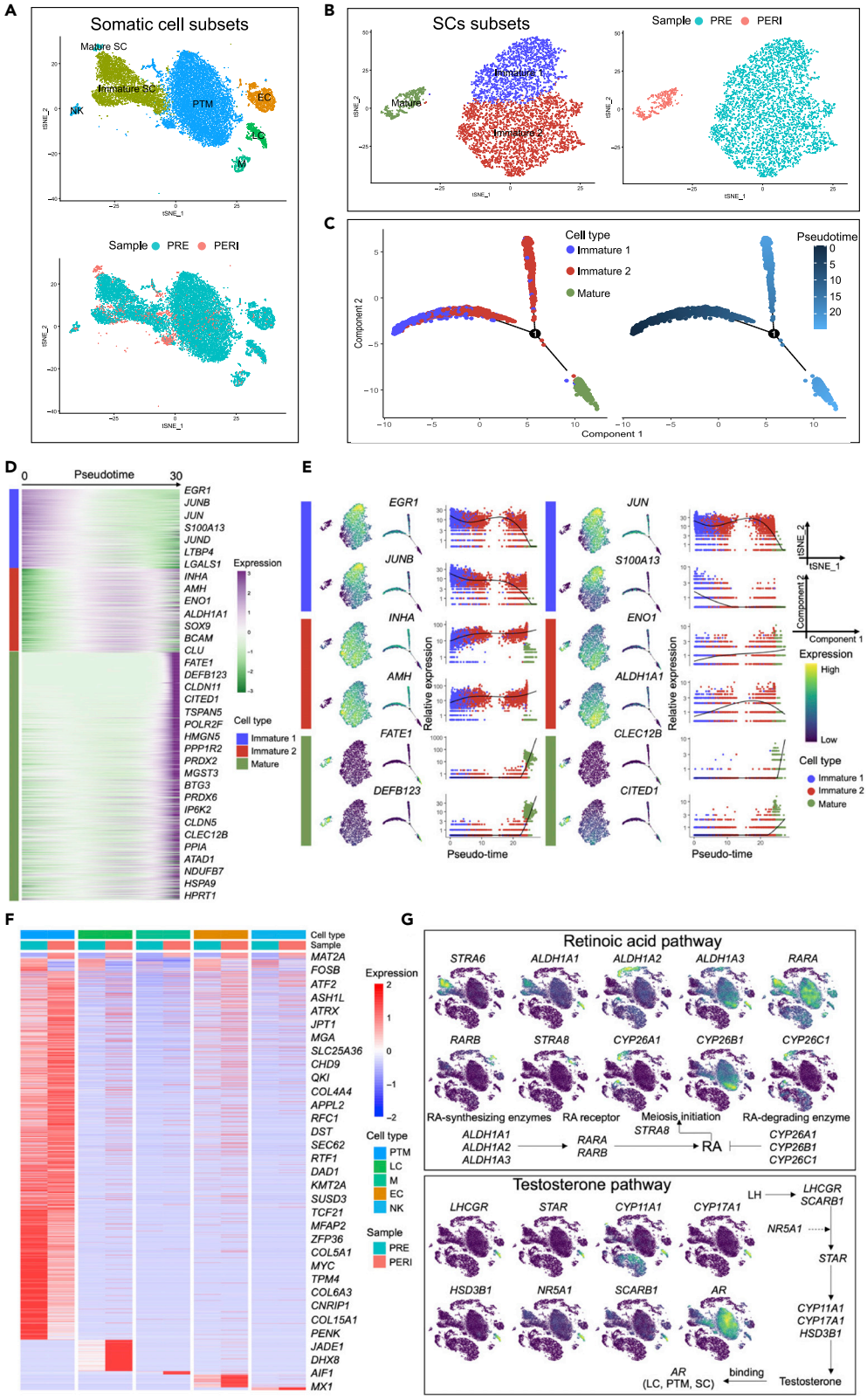
A
Somatic cell subsets
Mature SC
Immature SC
PTM
EC
NK
LC
M
Sample PRE PERI
B
SCs subsets
Immature 1
Immature 2
Mature
Sample PRE PERI
C
Cell type
Immature 1
Immature 2
Mature
Pseudotime
Component 1
Component 2
D
Pseudotime
EGR1
JUNB
JUN
S100A13
JUND
LTBP4
LGALS1
INHA
AMH
ENO1
ALDH1A1
SOX9
BCAM
CLU
FATE1
DEFB123
CLDN11
CITED1
TSPAN5
POLR2F
HMGN5
PPP1R2
PRDX2
MGST3
BTG3
PRDX6
IP6K2
CLDN5
CLEC12B
PPIA
ATAD1
NDUFB7
HSPA9
HPRT1
Expression
Cell type
Immature 1
Immature 2
Mature
E
Relative expression
Pseudo-time
Expression
High
Low
Cell type
Immature 1
Immature 2
Mature
F
Cell type
Sample
MAT2A
FOSB
ATF2
ASH1L
ATRX
JPT1
MGA
SLC25A36
CHD9
QKI
COL4A4
APPL2
RFC1
DST
SEC62
RTF1
DAD1
KMT2A
SUSD3
TCF21
MFAP2
ZFP36
COL5A1
MYC
TPM4
COL6A3
CNRIP1
COL15A1
PENK
JADE1
DHX8
AIF1
MX1
Expression
Cell type
PTM
LC
M
EC
NK
Sample
PRE
PERI
G
Retinoic acid pathway
STRA6
ALDH1A1
ALDH1A2
ALDH1A3
RARA
RARB
STRA8
CYP26A1
CYP26B1
CYP26C1
RA-synthesizing enzymes
RA receptor
Meiosis initiation
RA-degrading enzyme
ALDH1A1
ALDH1A2
ALDH1A3
RARA
RARB
RA
STRA8
CYP26A1
CYP26B1
CYP26C1
Testosterone pathway
LHCGR
STAR
CYP11A1
CYP17A1
HSD3B1
NR5A1
SCARB1
AR
LH
LHCGR
SCARB1
NR5A1
STAR
CYP11A1
CYP17A1
HSD3B1
AR
(LC, PTM, SC)
binding
Testosterone

Figure 6. Characterization of buffalo somatic lineages

(A) tSNE plot of somatic cell subsets in prepubertal and pubertal buffalo testes, colored by cell type (up) and sample (down).

(B) Re-clustering tSNE plot of SC lineages in buffalo testes, colored by cell type (left) and sample (right).

(C) Pseudotime trajectories of buffalo SCs subsets, coloring by cell type (left) and pseudotime value (right), respectively.

(D) Heatmap showing DEGs (q-value < 0.01) expression (rows) along the pseudotime (columns) axis.

(E) Feature plots, transcriptional trajectory plots, and pseudotime trajectory expression patterns of selected genes in Immature 1, Immature 2, and Mature clusters.

(F) Heatmap of differential genes in buffalo somatic cells (PTM, LC, M, EC, and NK) split by samples (PRE and PERI).

(G) tSNE plots showing gene relative expression levels of retinoic acid (up) and testosterone pathways (down).

pseudotime developmental axis, genes such as *EGR1*, *JUNB*, *JUN*, and *S100A13* showed elevated expression in the Immature 1 cluster and decreased expression with SC differentiation. Also, *INHA* and *AMH* broadly marked Immature SC, whereas expression was significantly higher in Immature 2 but negative for the Mature cluster, and genes with similar patterns included *ENO1*, *ALDH1A1*, *CLU*, and *BCAM*. Mature cluster specifically expressed *FATE1*, *DEFB123*, *CLEC12B*, *CITED1*, and *TSPAN5* (Figures 6D and 6E). Notably, mitochondrial function was enhanced along with the pseudotime developmental differentiation of SCs (Figures S6D and S6E and Table S5).

Heatmap showing the expression patterns of prepubertal and pubertal somatic cell marker genes. (Figure 6F and Table S7). Afterward, the focus was only on the expression of several paracrine factors, cytokines, growth factors, and ligand-receptor genes which have been associated with spermatogenesis. For instance, some immune-related factors such as interleukin (IL) 1 (*IL1A* and *IL1B*) and *CSF1* were specifically secreted by M cells in buffalo. *AMH*, inhibin (*INHA* and *INHBB*), and desert hedgehog signaling molecule (*DHH*) are produced by SCs; moreover, *DHH* and *AMH* are the essential downstream gene of SRY (sex determining region Y)-box9 (*SOX9*).[87] As expected, *DHH* and *INHBB* were expressed specifically in Immature SC and Mature SC; *AMH* and *INHA* were only expressed in Immature SC. Remarkably, many cytokines and hormones require to bind with their receptors to function, and we still found expression patterns of some ligand-receptor signaling pathways, such as *CLCL12-CXCR4*, *KITLG-KIT*, and *CGA-FSHR* (Figure S6F). These findings further suggested that the somatic cells also form strong interactions to create a microenvironment for spermatogenesis.

Retinoic acid (RA) is essential for male spermatogonial development and spermatocyte meiosis in both humans and mice.[54,88] Importantly, the membrane receptor *STRA6*, which is responsible for the intake of retinol, was specifically expressed in SCs (Immature 2) of buffalo testes. Similarly, *ALDH1A2* was expressed from pachytene to diplotene spermatocytes in postnatal mouse testes.[89] *In situ* hybridization showed that the RA-degrading enzyme *CYP26B1* was only expressed in PTM cells in mice,[89] but its transcript was detected in both buffalo SCs (Immature 1) and PTM cells *ALDH1A1* transcripts were found in immature SC (Immature 1 and Immature 2) and LC, and *ALDH1A3* was found in SCs (Immature 1 and Mature), PTM, and LC, suggesting that buffalo LC and PTM cells participated in RA synthesis. As for RA receptors, *RARA* was predominantly expressed in SSC-1 (*NANOS2*$^{+}$/*GFRA1*$^{+}$), SCs (Immature 1, Immature 2, and Mature), and PTM cells, but was only weakly expressed in LC, EC, and M. *RARB* was more abundant in SPG subsets (SSC-1, SSC-2, and Diff.ing SPG) and pre.L primary spermatocytes. These findings suggested that SCs, PTM, LC, EC, and M are involved in the RA regulation of spermatogonial differentiation (*NANOS2*$^{+}$/*GFRA1*$^{+}$) and meiotic initiation in buffalo (Figures 6G and S6G).

Testicular endocrine function is accomplished by androgen biosynthesis by LCs.[90] Testosterone is one of the major representative androgens regulating spermatogenesis in mammals by binding to the androgen receptor (*AR*).[91,92] Here, steroidogenesis-related genes were specifically expressed in LC. *AR* was expressed in LC, PTM, and SC in buffalo testes but negative for germline cells, suggesting that testosterone promotes spermatogenesis by the interactions among LC, PTM, and SC (Figure 6G).

Testicular cell-cell communication

Significant differences were observed in the number and strength of interactions (secreted signaling) among different testicular cell populations (Figure 7A and Table S8), with prepubertal cells showing a higher overall strength of interactions than pubertal cells, as evidenced by interactions between somatic cells (Figures S7A and S7B). Comparing the overall information flow of each signaling pathway revealed 17 signaling pathways, with PRE- and PERI-derived cells sharing four signaling pathways (PTN, MK, IGF,

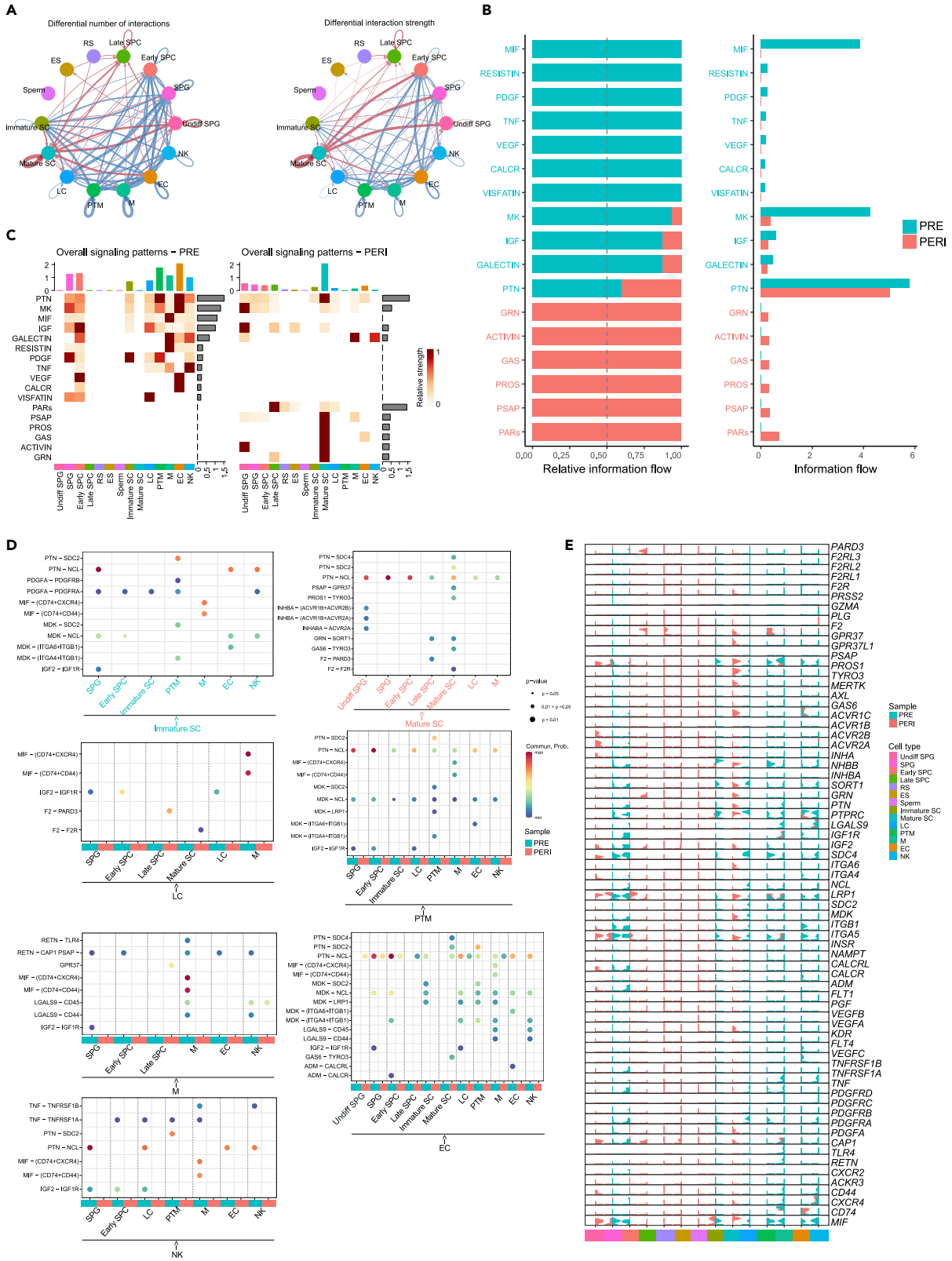
A
Differential number of interactions
Differential interaction strength
RS
Late SPC
Early SPC
ES
SPG
Sperm
Undiff SPG
Immature SC
NK
Mature SC
EC
LC
PTM
M
B
MIF
RESISTIN
PDGF
TNF
VEGF
CALCR
VISFATIN
MK
IGF
GALECTIN
PTN
GRN
ACTIVIN
GAS
PROS
PSAP
PARs
Relative information flow
Information flow
PRE
PERI
C
Overall signaling patterns – PRE
Overall signaling patterns – PERI
Relative strength
D
Immature SC
Mature SC
LC
PTM
M
EC
NK
p-value
Commun. Prob.
Sample
PRE
PERI
E
Sample
Cell type
Undiff SPG
SPG
Early SPC
Late SPC
RS
ES
Sperm
Immature SC
Mature SC
LC
PTM
M
EC
NK

Figure 7. Global testicular cell-cell communication network in buffalo

(A) Number of interactions and interaction strength among all testicular cell types.

(B) Overall information flow of each signaling pathway from PRE and PERI.

(C) Heatmap comparison of overall signaling in PRE- and PERI-derived testicular cells.

(D) Overview of ligand-receptor interactions (p-value < 0.05) of buffalo testicular cells. The size of the circle represents the p-value, with red representing the communication probability, whereas the color of the square represents the sample resource, with turquoise representing PRE and red representing PERI.

(E) Violin plots showing the expression of ligand-receptor pairs split by sample.

and GALECTIN) (Figure 7B). Notably, Mature SC was placed at the center of testicular intercellular communication, occupying the strongest signaling sender and receiver of five signaling pathways (GRN, GAS, PROS, PSAP, and PTN). Meanwhile, in the ACTIVIN pathway that promotes spermatogenesis,[93] cell-cell communication was only from Mature SC to Undiff SPG (Figures 7C, S7C, and S7D).

Furthermore, ligand-receptor pairs that function in the signaling pathway were examined, and somatic cells were found to interact with somatic/germ cells by paracrine/autocrine signaling (Figure 7D and Table S9). Especially, Undiff SPG majorly expressed receptors of the ACTIVIN (*ACVR1B* and *ACVR2A*) and PTN (*NCL*) pathway, whereas prepubertal spermatogonia were primarily represented by receptors of the IGF, MK, PDGF, PTN, and RESISTIN pathways—*IGF1R*, *NCL*, *PDGFRA*, *NCL*, and *CAP1*, respectively. Therefore, somatic cells might communicate with SSC by secreted signaling to maintain self-renewal or differentiation.

Simultaneously, prepubertal testicular somatic cell communication was predominantly clustered in the IGF, MIF, MK, PTN, GALECTIN, RESISTIN, CALCR, and TNF pathways, whereas pubertal cells were concentrated in PARs, GALECTIN, PSAP, GAS, and PTN pathways. *PTPRC* (*CD45*) was increased in abundance in M and NK cells of PERI, demonstrating that the GALECTIN pathway is involved in *PTPRC*$^{+}$ cell proliferation, differentiation, angiogenesis (formed by EC expressing ligand *LGALS9*), and immune response during buffalo testis development[94,95] (Figures 7E and S7E). Briefly, our data showed similarities and dissimilarities of microenvironments in prepubertal and pubertal spermatogenic cells, provided evidence for understanding cellular interactions during spermatogenesis, and highlighted the mechanisms of stem cell maintenance.

DISCUSSION

In mammals, male fertility requires the coordination of endocrine and exocrine testicular functions (androgen secretion and spermatogenesis), both of which are directly controlled by the hypothalamic-pituitary-gonadal (HPG) axis.[17,26,28,96] This study presents a comprehensive high-precision single-cell transcriptional cell atlas during spermatogenesis in buffalo, elucidating a gene expression roadmap and critical molecular markers for testicular cell development. In summary, scRNA-seq analysis was used to reveal sequentially distinct molecular events in spermatogenic cells and cell-cell communication mechanisms in the buffalo spermatogenic microenvironment, which can establish molecular foundations for the cultivation of germline stem cells *in vitro*, organoid culture, and agricultural superior livestock breeding.

Categorization of testicular germ and somatic cells

Spermatogenic cells were distinguished from microenvironment somatic cells according to *DDX4*- and *VIM*-positive expression[32,97] (Figures 1E, S1C, and S1D). Adult SSCs in mice were reported to compose only 0.03% of total germ cells.[98,99] Similarly, the undifferentiated SPG (buffalo) consisted of PERI only (42 cells), which expressed many identified markers such as pluripotency TFs (*SALL4* and *ETV5*), *ELAVL2*, and *PIWIL4*.[28,33,97,100,101] A recent spermatogenesis scRNA-seq study that failed to mark adult SSCs in sheep highlights the challenge of identifying SSCs in domestic animals.[31] Notably, GO enrichment revealed that DEGs were primarily involved in gene expression, chromosome organization, and RNA processing, and these biological processes were enriched in SSC-related TFs (*TCF3* and *ZBTB16*),[29] ARID domain-containing proteins (KDM family) and epigenetic modifiers (*DNMT3A*),[102] and RNA processing factors (LSM, RBM, and SNRP families). It showed that the buffalo undifferentiated SPG most likely contained a population of SSCs responsible for maintenance and self-renewal, which was consistent with previous findings in humans and mice.[39,102]

SPG (PRE: 558 cells; PERI: 26 cells) were labeled by genetic markers in spermatogonial differentiation such as *NR6A1*, *FGFR3*, and *FMR1*, which were also commonly highly expressed in spermatogonial cells of

humans and mice.[27,29,39] SPG was shown to be predominantly involved in chromosome organization, RNA splicing, and cell cycle processes, with genes promoting SSC self-renewal (*UCHL1*, *UTF1*, *CHD1*, *FOXO1*, and *BMI1*) and spermatogonial proliferation expansion signals (*DMRT1*, *SOHLH1*, *KIT*, *TKTL1*, and *ESX1*).[36,103–105] These observations suggested that SPG was a mixed cluster of spermatogonia with multiple differentiation states and required further re-clustering for identification.

For the spermatocytes, Early SPC was marked by *TEX12*, *SMCHD1*, and *PRSS50*.[27,65,106] Late SPC was labeled by synaptonemal complex central element protein 2 (*SYCE2*), DAZ gene family member (*BOLL*), and mutL homolog 1 (*MLH1*).[55,107] In cynomolgus macaque testes, the single-cell analysis showed that *IZUMO4* is expressed in round spermatids,[97] and *TEX29* is expressed in the early spermatid stage.[26] Moreover, studies have shown that *ODF1*, *ODF2*, *ODF3*, *OAZ3*, and *AKAP4* are sperm tail-related genes, supporting the initial classification of haploid spermatids (RS, ES, Sperm).[77,108] In summary, buffalo prepubertal and pubertal testicular germ cells were defined at the single-cell level (multiple differentiation states existed within a cluster in the initial classification). Nonetheless, genetic markers and expression profiles specifically for seven germ cell stages were found to characterize spermatogenesis (Table S1).

Microenvironment somatic cells (*VIM*+) secrete multiple cytokines, growth factors, hormones, and paracrine factors participating in the regional regulatory mechanism of spermatogenesis, and spermatogenesis depends on the maturity of somatic cells.[5,96,109] The differential expression of *AMH* and *CLDN11* in the original classification categorized SCs into two distinct cell clusters, despite the lack of a suitable marker to represent the overall status of SCs (Immature SC and Mature SC).[109] The prepubertal male mammalian SC is predominantly characterized by anti-Müllerian hormone (AMH), which lacks androgen receptor expression, and lacks the blood-testis barrier (BTB) as well.[110] The appearance of *CLDN11* transcripts signals that SCs entered the mature stage, which is characterized by loss of proliferation activity, BTB formation, and providing nutritional and structural support to germ cells at all developmental stages of spermatogenesis.[11,111] *KITLG* (KIT ligand, stem cell factor) plays a distinct role in regulating the fate of mouse spermatogonia.[112,113] The maturation roadmap of SCs was demonstrated by pseudotime trajectory analysis, and the time of *KITLG* expression initiation in buffalo SCs was found to be the same as *SOX9*, indicating a potential regulatory relationship that requires further verification. Specifically, *SHBG*, rather than *SOX9*, *WT1*, or *GATA4*, was a more comprehensive molecular marker for prepubertal and pubertal SCs in buffalo. The buffalo PTM expressed DHH receptor (*PTCH1*), PDGF receptor (*PDGFRA*), and *AR*, indicating that it interacts with other somatic cells to mediate spermatogenesis by participating in hedgehog, PDGF, and androgen signaling pathways. These results corroborate the findings of a previous study on humans.[67]

In the interstitial compartment of buffalo testis, LC specifically expressed testosterone biosynthesis-related genes (*STAR*, *HSD3B1*, *CYP17A1*, *CYP11A1*, and *NR5A1*), which match those observed in earlier studies.[114,115] High expression levels of *AR* in buffalo SC, PTM, and LC indicated that androgen signaling promotes sex differentiation, gonadal development, and spermatogenesis by the cooperative work of SC, PTM, and LC, with androgen signaling being subsequently transmitted to germ cells by SC.[116] Furthermore, weak *AR* expression was observed in buffalo EC (*PECAM*$^+$/*CLDN5*$^+$/*ECSCR*$^+$), which was consistent with previous observations that testosterone interacts with EC.[117] In addition, two classes of *PTPRC*$^+$ cells—M (*CSF1R*$^+$/*CD74*$^+$/*MAFB*$^+$) and NK (*PTPRC*$^+$/*NKG7*$^+$/*KLRF1*$^+$/*CD94*+)—were identified. M is a "niche" in the interstitial compartment of prepubertal and adult mice SSCs, interacting with LCs to promote steroid synthesis, expressing the SPG proliferation and differentiation-inducing molecule *CSF1*, and still being involved in the RA biosynthetic pathway.[118] IF staining of adult mouse testis revealed that *CSF1* was expressed in LC, PTM, and M, whereas *CSF1R* was expressed in spermatogonial cells.[118,119] Conversely, we found that *CSF1* and *CSF1R* were specifically expressed in M in the present study. Therefore, *CSF1* is unlikely to influence the proliferation or self-renewal of SSC by binding to *CSF1R* in buffalo.

Spermatogenic cell development

Re-clustering analysis was performed on the original cluster to identify highly variable genes for cell fate transition between neighboring spermatogenic cells. SSC-1 (*NANOS2*$^+$/*GFRA1*$^+$) differentiated the earliest in the cell trajectory analysis of SPG subsets, expressing receptors (*GFRA1* and *RET*), and transcription factors (*ETV5*) associated with the GDNF signaling pathway. Thus, the GDNF signaling pathway is required to maintain SSC self-renewal in buffalo, similar to mice, rats, and humans.[33,101,120] SSC-2 (*PIWIL4*$^+$/*FOXO1*$^+$) specifically expresses *PRC1*, *BMI1*, and *TAF4B*. In particular, *ZBTB16* and *TAF4B* were found to be under differential signaling control in prepubertal human spermatogonia and mouse SSC, which might

prevent differentiation without being directly involved in self-renewal.[33] Moreover, human SSEA4$^+$ SSCs had high transcript levels of *PRC1* and *BMI1*.[39] *DMRT1* is expressed in mouse SCs and spermatogonia (all stages) and promotes spermatogonial differentiation by activating *SOHLH1* and inhibits meiotic initiation by specific interruption of *STRA8* transcription (RA pathway).[121] Similarly, the scRNA-seq profile revealed that *DMRT1* and *SOHLH1* simultaneously marked Diff.ing SPG, and *STRA8* initiated weak expression in Diff.ed SPG (*IRF1*$^+$/*KLF4*$^+$), peaking in L primary spermatocytes.

Compared with other mammals, buffalo shared some conserved SSCs, such as *UCHL1*, *UTF1*, *ZBTB16*, *DAZL*, *SOX4*, *NANOS2*, *GFRA1*, *PAX7*, *SALL4*, *ITGA6*, *RET*, *PIWIL4*, *FOXO1*, *MORC1*, *TAF4B*, *NR6A1*, and *FGFR3*.[27,97] Nevertheless, few identified SSC markers were not detected in buffalo, including *NGN3*, *PLPPR3*, *TSPAN33*, *GPR125*, *SSEA4*, *MAGEA4*, *DPPA4*, *BCL6B*, and *FOXO3*.[26,29,122,123] Of interest, *RBM47* and *SLPI* were shown to be specifically expressed in mouse primordial germ cells (PGCs).[124] In contrast, *NANOS2*, which is similar to *SLPI*, was particularly expressed in SSC-1 in the present study, whereas *RBM47* was specifically expressed in SSC-2. The earlier systematic investigation of spermatogonial cell subtypes in the domestic animal field came from a single-cell examination of a 150-day-old Guanzhong pig.[32] In short, this detailed characterization of the single-cell transcriptional atlas of buffalo spermatogonia can contribute to theoretical models of spermatogonial development in livestock.

Spermatogonial mitotic division and differentiation into pre.L spermatocytes all occur in the basal compartment, whereas other spermatocytes and post-meiotic spermatids are separated in the adluminal compartment.[125] Increasing advancements in scRNA-seq allowed for the classification of spermatocytes into more specialized stages, and a recent study reported 12 phases of spermatocytes during mouse spermatogenesis and listed the following stages: G1, ePL, mPL, and lPL (preleptotene stage), L, Z, eP, mP, lP, D, MI, and MII stage.[38] Likewise, our data showed the following spermatocyte subtypes: pre.L (*REC8*$^+$/*SMC3*$^+$), L (*SYCP3*$^+$/*ZCWPW1*$^+$), Z (*SYCP1*$^+$/*TEX101*$^+$), eP (*PIWIL1*$^+$/*CCDC112*$^+$), mP (*HORMAD2*$^+$/*REC114*$^+$), lP (*NME5*$^+$/*NME8*$^+$), D (*AURKA*$^+$/*AURKB*$^+$) and MI-II (*SUN5*$^+$/*FZR1*$^+$) (Figures 3 and S3). Multiple interspecies conserved spermatocyte phase-specific markers were identified using scRNA-seq, including *ZCWPW1*, *TEX101*, *PIWIL1*/*CCDC112*, and *AURKA*/*SPATA16*, which broadly marked L, Z, P, and D primary spermatocytes, respectively, in human, mouse, monkey, pig, sheep, and buffalo.[64] Several unconserved genetic markers were observed in buffalo, presumably because the cycle of seminiferous epithelium differs among animals. Human, cynomolgus macaque, and mouse showed *DMRTB1* expression in differentiated spermatogonia, whereas *DMRTB1* expression was detected in pre.L spermatocytes in buffalo.[97] *HERC5* was highly expressed in human late primary spermatocytes,[27] whereas it was detected in the buffalo pre.L cluster. Similarly, *SYCP3* was expressed in mouse Z spermatocytes,[64] but was expressed in the buffalo L stage. To form species-specific maturing spermatozoa, round spermatids undergo a series of morphological transformations and chromatin remodeling.[77] Dynamic transcriptional signatures of buffalo spermiogenesis were revealed in the present study, and the major stage of histone-to-protamine chromatin remodeling was found to occur at the ES2 stage.

To improve understanding of male germ cells, detailed information on TMHMM-predicted proteins is provided in Table S6. The surface marker *ST3GAL2* has been identified as specific to prepubertal SSC in buffalo. Several other surface genes were selected as candidate markers for the buffalo spermatogenic lineage, such as *ITGA6*, *KNTC1*, *RHOA*, and *ITGB5* (Figure 5C). Furthermore, it would be interesting to explore the process of transforming germ cell fate during puberty based on cell surface markers isolating single-cell-defined testicular germ cells *in vitro*. Hence, single-cell transcriptome analysis was used to define the dynamic transformation of spermatogenesis in buffalo, thereby contributing to deepening our understanding of the regulatory basis of male germ cell development.

Global testicular cell-cell communication network in buffalo

SSCs undergo spermatogenesis in a microenvironment created by testicular somatic cells, a complex process that involves self-renewal and differentiation into spermatozoa.[21] Nevertheless, the mechanism of mammalian testicular cell communication in the physiological state is poorly defined. In addition to examining the expression distribution of paracrine factors (e.g., *DHH*, *NRG1*, *POMC*, and *INSL3*), cytokines (e.g., *IL1A*, *IL1B*, *CSF1*, and *INHBB*), growth factors (e.g., *IGF2*, *TGFβs*, *PDGFs*, *HGF*, *FGF1*, *VEGFA*, and *NGF*), CXCL12/CXCR4 signaling, KITLG/KIT signaling, RA biosynthetic pathway, and testosterone pathway (Figures 6G, S6F, and S6G), global paracrine/autocrine signaling interactions were observed between prepubertal and pubertal buffalo testicular cells by CellChat analysis (Figures 7 and S7). Of note, the limitation

of CellChat is that high expression of ligands and receptors at the RNA level does not necessarily correlate with actual cell-cell signaling because cell signaling occurs at the protein level.[126] Nevertheless, CellChat analysis is still a good indicator for detecting potential signaling pathways in intercellular communication.

During the information flow from niche cells to sender cells, the IGF pathway was detected in the interaction pattern of prepubertal somatic cells (Immature SC, LC, PTM, M, EC, and NK). Of interest, germ cells (Undiff SPG, SPG, and Early SPC) also expressed *IGF2*, and the IGF pathway was evident in the flow of information from germ cells to niche cells. Thus, the data further supported that IGF is the most critical positive regulator of immature SC proliferation, promoting the proliferation, differentiation, and development of PTM, LC, EC, M, and NK cells.[127] Meanwhile, the IGF pathway communicates bidirectionally between germ and niche cells. The PDGF pathway enhances steroid production in LC, promotes PTM contractions, and stimulates germ cell differentiation and proliferation.[128,129] Similarly, *PDGFA* showed specific expression in buffalo SCs, and PDGF receptors (*PDGFRA* and *PDGFRB*) were predominantly expressed in Immature SC and PTM, and slightly expressed in LC. The buffalo PDGF signaling pathway was regulated by PDGF/PDGFR during testis development by the interaction of SC, PTM, and LC. Furthermore, although ACTIVIN receptors (*ACVR2A* and *ACVR1B*) were expressed in both prepubertal and pubertal-derived SPGs in buffalo, the ACTIVIN communication signal was only detected in adult buffalo when the sender cell is adult SC and the receiver cell is mature SC. Hence, the data further confirmed that the ACTIVIN pathway promotes the expansion of spermatogonia in adult mammals (including humans and mice).[130]

M-specific secreted immune-related cytokines, IL1 (*IL1A* and *IL1B*) in prepubertal and pubertal buffalo, whereas IL1A is secreted by SC in humans and rats, and has a direct effect on germ cell differentiation and testicular steroid hormone production.[131,132] The GALECTIN pathway was found in buffalo EC and *PTPRC*$^{+}$ immune cells (M and NK), confirming a crucial role in angiogenesis and the maintenance of an immunologically privileged environment in the testis.[94] Importantly, *TNF* is a pro-inflammatory cytokine produced by SC and LC, which increases the secretion of transferrin in SC.[133] However, only *TNF* and its receptor *TNFRSF1B* were detected in buffalo M and NK cells, whereas *TNFRSF1A* was present mainly in PTM, LC, M, immature SC, and EC. The results indicate that *TNF* was mainly expressed in immune cells of buffalo testis and functioned as a signaling cascade by cellular communication.

Several ligands share the same receptor, demonstrating that paracrine factors most likely crosstalk between multiple signals. For instance, *MDK* (MK pathway) and *PTN* (PTN pathway) share three receptors (*NCL*, *SDC2*, and *SDC4*); *F2* and *PLG* (PARs pathway) share two receptors *F2R* and *PARD3*; *MIF* (MIF pathway) and *LGALS9* (GALECTIN pathway) share receptor *CD44*; and *GAS6* (GAS pathway) and *PROS1* (PROS pathway) share receptor *TYRO3*. Our data further supported that the MK/PTN family promotes angiogenesis[134] and found that *NCL* was also expressed in germ cells (Undiff SPG, SPG, Early SPC, and Late SPC), indicating that the MK/PTN family was also involved in constructing the "microenvironment" of buffalo spermatogenesis. The role of angiogenic signaling in maintaining self-renewal in SSCs is yet to be evaluated functionally, which is worthy of further investigation. In short, the paracrine/autocrine signaling interactions in prepubertal and pubertal buffalo testicular cells that create distinct spermatogenic microenvironments were elucidated, yielding a potential ligand-receptor list for establishing germline stem cells and organoid culture *in vitro*.

This study establishes a single-cell transcriptional atlas of prepubertal and pubertal healthy buffalo testes, uncovering dynamic and complex processes in the sequential cell fate transition from SSCs to spermatozoa and developmental trajectory of microenvironment somatic cells during spermatogenesis. Also, this study presents a global buffalo testicular cell-cell communication network that maintains regular spermatogenesis under physiological conditions. Overall, our dataset provides comprehensive, distinctive, and valuable information on buffalo spermatogenesis and contributes to the molecular basis for studies of the male germline from livestock models *in vitro*.

Limitations of the study

The present study focused on scRNA-seq analysis and IF staining of key markers in the testis. However, further experimental validation is required for the expression and localization of novel markers, because commercial antibodies do not easily function in buffalo. Only the single-cell data of prepubertal and pubertal buffalo testes was compared, which does not entirely reveal the gradual molecular process of the

testis from prepuberty to puberty. Further studies using sequencing data from multiple continuous development samples may reveal additional details. Besides, integrating multi-species single-cell data to investigate spermatogenesis contributes to enhancing our understanding of male fertility and spermatogenesis. Although two SSC clusters were identified in the present study without performing functional assays, further studies involving the isolation of SSC xenografts by cell surface markers can improve the current findings.

STAR★METHODS

Detailed methods are provided in the online version of this paper and include the following:

- KEY RESOURCES TABLE
- RESOURCE AVAILABILITY
  - Lead contact
  - Materials availability
  - Data and code availability
- EXPERIMENTAL MODEL AND SUBJECT DETAILS
- METHOD DETAILS
  - Buffalo testes sample preparation
  - 10x genome library preparation and sequencing
  - Genome alignment and gene expression quantification
  - Cell clustering and annotation
  - Single-cell trajectory analysis
  - Prediction of transmembrane (TM) helices in proteins
  - Comparison analysis of PRE- and PERI-derived testicular cells using CellChat
  - Hematoxylin and eosin staining
  - Immunostaining of buffalo testicular tissue
- QUANTIFICATION AND STATISTICAL ANALYSIS

SUPPLEMENTAL INFORMATION

Supplemental information can be found online at https://doi.org/10.1016/j.isci.2022.105733.

ACKNOWLEDGMENTS

This work was supported by the National Natural Science Foundation of China (Grant No. 32160789).

AUTHOR CONTRIBUTIONS

Conceptualization: L.F.H. and J.J.Z.

Methodology: L.F.H., J.J.Z., and X.C.H.

Investigation: L.F.H., P.F.Z., W.H.Y., R.F.L., and Q.Q.S.

Visualization: L.F.H., J.J.Z., and P.F.Z.

Funding acquisition: M.Z.

Project administration: M.Z.

Supervision: M.Z., Q.F., and Y.Q.L.

Writing – original draft: L.F.H.

Writing – review and editing: M.Z. and Q.F.

DECLARATION OF INTERESTS

The authors declare no competing interests.

Received: June 17, 2022
Revised: October 24, 2022
Accepted: December 1, 2022
Published: January 20, 2023

REFERENCES

1. Perera, B.M.A.O. (2011). Reproductive cycles of buffalo. Anim. Reprod. Sci. *124*, 194–199. https://doi.org/10.1016/j.anireprosci.2010.08.022.

2. Michelizzi, V.N., Dodson, M.V., Pan, Z., Amaral, M.E.J., Michal, J.J., McLean, D.J., Womack, J.E., and Jiang, Z. (2010). Water buffalo genome science comes of age. Int. J. Biol. Sci. *6*, 333–349. https://doi.org/10.7150/ijbs.6.333.

3. D'Occhio, M.J., Ghuman, S.S., Neglia, G., Della Valle, G., Baruselli, P.S., Zicarelli, L., Visintin, J.A., Sarkar, M., and Campanile, G. (2020). Exogenous and endogenous factors in seasonality of reproduction in buffalo: a review. Theriogenology *150*, 186–192. https://doi.org/10.1016/j.theriogenology.2020.01.044.

4. Khatun, M., Kaur, S., Kanchan, and Mukhopadhyay, C.S. (2013). Subfertility problems leading to disposal of breeding bulls. Asian-Australas. J. Anim. Sci. *26*, 303–308. https://doi.org/10.5713/ajas.2012.12413.

5. Oatley, J.M., and Brinster, R.L. (2012). The germline stem cell niche unit in mammalian testes. Physiol. Rev. *92*, 577–595. https://doi.org/10.1152/physrev.00025.2011.

6. McGowan, M., Holland, M.K., and Boe-Hansen, G. (2018). Review: ontology and endocrinology of the reproductive system of bulls from fetus to maturity. Animal *12*, s19–s26. https://doi.org/10.1017/S1751731118000460.

7. Law, N.C., Oatley, M.J., and Oatley, J.M. (2019). Developmental kinetics and transcriptome dynamics of stem cell specification in the spermatogenic lineage. Nat. Commun. *10*, 2787. https://doi.org/10.1038/s41467-019-10596-0.

8. Staub, C., and Johnson, L. (2018). Review: spermatogenesis in the bull. Animal *12*, s27–s35. https://doi.org/10.1017/S1751731118000435.

9. Griswold, M.D. (1998). The central role of Sertoli cells in spermatogenesis. Semin. Cell Dev. Biol. *9*, 411–416. https://doi.org/10.1006/scdb.1998.0203.

10. Bhang, D.H., Kim, B.-J., Kim, B.G., Schadler, K., Baek, K.-H., Kim, Y.H., Hsiao, W., Ding, B.-S., Rafii, S., Weiss, M.J., et al. (2018). Testicular endothelial cells are a critical population in the germline stem cell niche. Nat. Commun. *9*, 4379. https://doi.org/10.1038/s41467-018-06881-z.

11. Tarulli, G.A., Stanton, P.G., and Meachem, S.J. (2012). Is the adult sertoli cell terminally differentiated? Biol. Reprod. *87*, 13. 1-11. https://doi.org/10.1095/biolreprod.111.095091.

12. Chen, S.R., and Liu, Y.X. (2015). Regulation of spermatogonial stem cell self-renewal and spermatocyte meiosis by Sertoli cell signaling. Reproduction *149*, R159–R167. https://doi.org/10.1530/REP-14-0481.

13. Tan, K., Song, H.-W., and Wilkinson, M.F. (2020). Single-cell RNAseq analysis of testicular germ and somatic cell development during the perinatal period. Development *147*, dev183251. https://doi.org/10.1242/dev.183251.

14. Bhushan, S., and Meinhardt, A. (2017). The macrophages in testis function. J. Reprod. Immunol. *119*, 107–112. https://doi.org/10.1016/j.jri.2016.06.008.

15. Barrio, R., de Luis, D., Alonso, M., Lamas, A., and Moreno, J.C. (1999). Induction of puberty with human chorionic gonadotropin and follicle-stimulating hormone in adolescent males with hypogonadotropic hypogonadism. Fertil. Steril. *71*, 244–248. https://doi.org/10.1016/s0015-0282(98)00450-6.

16. Skinner, M.K. (1991). Cell-cell interactions in the testis. Endocr. Rev. *12*, 45–77. https://doi.org/10.1210/edrv-12-1-45.

17. Rawlings, N., Evans, A.C.O., Chandolia, R.K., and Bagu, E.T. (2008). Sexual maturation in the. Bull. Reprod. Domest. Anim. *43*, 295–301. https://doi.org/10.1111/j.1439-0531.2008.01177.x.

18. Neto, F.T.L., Bach, P.V., Najari, B.B., Li, P.S., and Goldstein, M. (2016). Spermatogenesis in humans and its affecting factors. Semin. Cell Dev. Biol. *59*, 10–26. https://doi.org/10.1016/j.semcdb.2016.04.009.

19. De Rooij, D.G. (2009). The spermatogonial stem cell niche. Microsc. Res. Tech. *72*, 580–585. https://doi.org/10.1002/jemt.20699.

20. Krausz, C., and Riera-Escamilla, A. (2018). Genetics of male infertility. Nat. Rev. Urol. *15*, 369–384. https://doi.org/10.1038/s41585-018-0003-3.

21. Sharma, S., Wistuba, J., Pock, T., Schlatt, S., and Neuhaus, N. (2019). Spermatogonial stem cells: updates from specification to clinical relevance. Hum. Reprod. Update *25*, 275–297. https://doi.org/10.1093/humupd/dmz006.

22. de Kretser, D.M., Loveland, K.L., Meinhardt, A., Simorangkir, D., and Wreford, N. (1998). Hum. Reprod. *13*, 1–8. https://doi.org/10.1093/humrep/13.suppl_1.1.

23. Wang, Y., and Navin, N.E. (2015). Advances and applications of single-cell sequencing technologies. Mol. Cell *58*, 598–609. https://doi.org/10.1016/j.molcel.2015.05.005.

24. Wang, X., He, Y., Zhang, Q., Ren, X., and Zhang, Z. (2021). Direct comparative analyses of 10X Genomics Chromium and smart-seq2. Dev. Reprod. Biol. *19*, 253–266. https://doi.org/10.1016/j.gpb.2020.02.005.

25. Guo, J., Sosa, E., Chitiashvili, T., Nie, X., Rojas, E.J., Oliver, E., DonorConnect, Plath, K., Hotaling, J.M., Stukenborg, J.B., et al. (2021). Single-cell analysis of the developing human testis reveals somatic niche cell specification and fetal germline stem cell establishment. Cell Stem Cell *28*, 764–778.e4. https://doi.org/10.1016/j.stem.2020.12.004.

26. Wang, M., Liu, X., Chang, G., Chen, Y., An, G., Yan, L., Gao, S., Xu, Y., Cui, Y., Dong, J., et al. (2018). Single-cell RNA sequencing analysis reveals sequential cell fate transition during human spermatogenesis. Cell Stem Cell *23*, 599–614.e4. https://doi.org/10.1016/j.stem.2018.08.007.

27. Guo, J., Grow, E.J., Mlcochova, H., Maher, G.J., Lindskog, C., Nie, X., Guo, Y., Takei, Y., Yun, J., Cai, L., et al. (2018). The adult human testis transcriptional cell atlas. Cell Res. *28*, 1141–1157. https://doi.org/10.1038/s41422-018-0099-2.

28. Guo, J., Nie, X., Giebler, M., Mlcochova, H., Wang, Y., Grow, E.J., DonorConnect, Kim, R., Tharmalingam, M., Matilionyte, G., et al. (2020). The dynamic transcriptional cell atlas of testis development during human puberty. Cell Stem Cell *26*, 262–276.e4. https://doi.org/10.1016/j.stem.2019.12.005.

29. Sohni, A., Tan, K., Song, H.-W., Burow, D., de Rooij, D.G., Laurent, L., Hsieh, T.-C., Rabah, R., Hammoud, S.S., Vicini, E., and Wilkinson, M.F. (2019). The neonatal and adult human testis defined at the single-cell level. Cell Rep. *26*, 1501–1517.e4. https://doi.org/10.1016/j.celrep.2019.01.045.

30. Shami, A.N., Zheng, X., Munyoki, S.K., Ma, Q., Manske, G.L., Green, C.D., Sukhwani, M., Orwig, K.E., Li, J.Z., and Hammoud, S.S. (2020). Single-cell RNA sequencing of human, macaque, and mouse testes uncovers conserved and divergent features of mammalian spermatogenesis. Dev. Cell *54*, 529–547.e12. https://doi.org/10.1016/j.devcel.2020.05.010.

31. Yang, H., Ma, J., Wan, Z., Wang, Q., Wang, Z., Zhao, J., Wang, F., and Zhang, Y. (2021). Characterization of sheep spermatogenesis through single-cell RNA sequencing. Faseb. J. *35*, e21187. https://doi.org/10.1096/fj.202001035RRR.

32. Zhang, L., Li, F., Lei, P., Guo, M., Liu, R., Wang, L., Yu, T., Lv, Y., Zhang, T., Zeng, W., et al. (2021). Single-cell RNA-sequencing reveals the dynamic process and novel markers in porcine spermatogenesis. J. Anim. Sci. Biotechnol. *12*, 122. https://doi.org/10.1186/s40104-021-00638-3.

33. Wu, X., Schmidt, J.A., Avarbock, M.R., Tobias, J.W., Carlson, C.A., Kolon, T.F., Ginsberg, J.P., and Brinster, R.L. (2009). Prepubertal human spermatogonia and mouse gonocytes share conserved gene expression of germline stem cell regulatory molecules. Proc. Natl. Acad. Sci. USA *106*, 21672–21677. https://doi.org/10.1073/pnas.0912432106.

34. Lukassen, S., Bosch, E., Ekici, A.B., and Winterpacht, A. (2018). Single-cell RNA sequencing of adult mouse testes. Sci. Data *5*, 180192. https://doi.org/10.1038/sdata.2018.192.

35. Grive, K.J., Hu, Y., Shu, E., Grimson, A., Elemento, O., Grenier, J.K., and Cohen, P.E. (2019). Dynamic transcriptome profiles within spermatogonial and spermatocyte populations during postnatal testis maturation revealed by single-cell sequencing. PLoS Genet. *15*, e1007810. https://doi.org/10.1371/journal.pgen.1007810.

36. Zhao, L., Yao, C., Xing, X., Jing, T., Li, P., Zhu, Z., Yang, C., Zhai, J., Tian, R., Chen, H., et al. (2020). Single-cell analysis of developing and azoospermia human testicles reveals central role of Sertoli cells. Nat. Commun. *11*, 5683. https://doi.org/10.1038/s41467-020-19414-4.

37. Green, C.D., Ma, Q., Manske, G.L., Shami, A.N., Zheng, X., Marini, S., Moritz, L., Sultan, C., Gurczynski, S.J., Moore, B.B., et al. (2018). A comprehensive roadmap of murine spermatogenesis defined by single-cell RNA-seq. Dev. Cell *46*, 651–667.e10. https://doi.org/10.1016/j.devcel.2018.07.025.

38. Chen, Y., Zheng, Y., Gao, Y., Lin, Z., Yang, S., Wang, T., Wang, Q., Xie, N., Hua, R., Liu, M., et al. (2018). Single-cell RNA-seq uncovers dynamic processes and critical regulators in mouse spermatogenesis. Cell Res. *28*, 879–896. https://doi.org/10.1038/s41422-018-0074-y.

39. Guo, J., Grow, E.J., Yi, C., Mlcochova, H., Maher, G.J., Lindskog, C., Murphy, P.J., Wike, C.L., Carrell, D.T., Goriely, A., et al. (2017). Chromatin and single-cell RNA-seq profiling reveal dynamic signaling and metabolic transitions during human spermatogonial stem cell development. Cell Stem Cell *21*, 533–546.e6. https://doi.org/10.1016/j.stem.2017.09.003.

40. Wrobel, K.H. (2000). Prespermatogenesis and spermatogoniogenesis in the bovine testis. Anat. Embryol. *202*, 209–222. https://doi.org/10.1007/s004290000111.

41. Mahla, R.S., Reddy, N., and Goel, S. (2012). Spermatogonial stem cells (SSCs) in buffalo (Bubalus bubalis) testis. PLoS One *7*, e36020. https://doi.org/10.1371/journal.pone.0036020.

42. Yoshida, S. (2016). From cyst to tubule: innovations in vertebrate spermatogenesis. Wiley Interdiscip. Rev. Dev. Biol. *5*, 119–131. https://doi.org/10.1002/wdev.204.

43. Boitani, C., Di Persio, S., Esposito, V., and Vicini, E. (2016). Spermatogonial cells: mouse, monkey and man comparison. Semin. Cell Dev. Biol. *59*, 79–88. https://doi.org/10.1016/j.semcdb.2016.03.002.

44. Lord, T., and Oatley, J.M. (2018). Functional assessment of spermatogonial stem cell purity in experimental cell populations. Stem Cell Res. *29*, 129–133. https://doi.org/10.1016/j.scr.2018.03.016.

45. Giassetti, M.I., Ciccarelli, M., and Oatley, J.M. (2019). Spermatogonial stem cell transplantation: insights and outlook for domestic animals. Annu. Rev. Anim. Biosci. *7*, 385–401. https://doi.org/10.1146/annurev-animal-020518-115239.

46. Fahrenkrug, S.C., Blake, A., Carlson, D.F., Doran, T., Van Eenennaam, A., Faber, D., Galli, C., Gao, Q., Hackett, P.B., Li, N., et al. (2010). Precision genetics for complex objectives in animal agriculture. J. Anim. Sci. *88*, 2530–2539. https://doi.org/10.2527/jas.2010-2847.

47. González, R., and Dobrinski, I. (2015). Beyond the mouse monopoly: studying the male germ line in domestic animal models. ILAR J. *56*, 83–98. https://doi.org/10.1093/ilar/ilv004.

48. Braun, R.E. (1998). Post-transcriptional control of gene expression during spermatogenesis. Semin. Cell Dev. Biol. *9*, 483–489. https://doi.org/10.1006/scdb.1998.0226.

49. Goel, S., Reddy, N., Mandal, S., Fujihara, M., Kim, S.-M., and Imai, H. (2010). Spermatogonia-specific proteins expressed in prepubertal buffalo (Bubalus bubalis) testis and their utilization for isolation and in vitro cultivation of spermatogonia. Theriogenology *74*, 1221–1232. https://doi.org/10.1016/j.theriogenology.2010.05.025.

50. Mikedis, M.M., Fan, Y., Nicholls, P.K., Endo, T., Jackson, E.K., Cobb, S.A., de Rooij, D.G., and Page, D.C. (2020). DAZL mediates a broad translational program regulating expansion and differentiation of spermatogonial progenitors. Elife *9*, e56523. https://doi.org/10.7554/eLife.56523.

51. Tian, H., Cao, Y.-X., Zhang, X.-S., Liao, W.-P., Yi, Y.-H., Lian, J., Liu, L., Huang, H.-L., Liu, W.-J., Yin, M.-M., et al. (2013). The targeting and functions of miRNA-383 are mediated by FMRP during spermatogenesis. Cell Death Dis. *4*, e617. https://doi.org/10.1038/cddis.2013.138.

52. Kanatsu-Shinohara, M., Lee, J., Inoue, K., Ogonuki, N., Miki, H., Toyokuni, S., Ikawa, M., Nakamura, T., Ogura, A., and Shinohara, T. (2008). Pluripotency of a single spermatogonial stem cell in mice. Biol. Reprod. *78*, 681–687. https://doi.org/10.1095/biolreprod.107.066068.

53. Jeong, H.-S., Bhin, J., Joon Kim, H., Hwang, D., Ryul Lee, D., and Kim, K.-S. (2017). Transcriptional regulatory networks underlying the reprogramming of spermatogonial stem cells to multipotent stem cells. Exp. Mol. Med. *49*, e315. https://doi.org/10.1038/emm.2017.2.

54. Griswold, M.D. (2016). Spermatogenesis: the commitment to meiosis. Physiol. Rev. *96*, 1–17. https://doi.org/10.1152/physrev.00013.2015.

55. Cahoon, C.K., and Hawley, R.S. (2016). Regulating the construction and demolition of the synaptonemal complex. Nat. Struct. Mol. Biol. *23*, 369–377. https://doi.org/10.1038/nsmb.3208.

56. Bhalla, N., and Dernburg, A.F. (2008). Prelude to a division. Annu. Rev. Cell Dev. Biol. *24*, 397–424. https://doi.org/10.1146/annurev.cellbio.23.090506.123245.

57. Page, S.L., and Hawley, R.S. (2003). Chromosome choreography: the meiotic ballet. Science *301*, 785–789. https://doi.org/10.1126/science.1086605.

58. Bolcun-Filas, E., and Handel, M.A. (2018). Meiosis: the chromosomal foundation of reproduction. Biol. Reprod. *99*, 112–126. https://doi.org/10.1093/biolre/ioy021.

59. Loidl, J. (2016). Conservation and variability of meiosis across the eukaryotes. Annu. Rev. Genet. *50*, 293–316. https://doi.org/10.1146/annurev-genet-120215-035100.

60. Zickler, D., and Kleckner, N. (2015). Recombination, pairing, and synapsis of homologs during meiosis. Cold Spring Harbor Perspect. Biol. *7*, a016626. https://doi.org/10.1101/cshperspect.a016626.

61. Hermann, B.P., Cheng, K., Singh, A., Roa-De La Cruz, L., Mutoji, K.N., Chen, I.-C., Gildersleeve, H., Lehle, J.D., Mayo, M., Westernströer, B., et al. (2018). The mammalian spermatogenesis single-cell transcriptome, from spermatogonial stem cells to spermatids. Cell Rep. *25*, 1650–1667.e8. https://doi.org/10.1016/j.celrep.2018.10.026.

62. Koubova, J., Menke, D.B., Zhou, Q., Capel, B., Griswold, M.D., and Page, D.C. (2006). Retinoic acid regulates sex-specific timing of meiotic initiation in mice. Proc. Natl. Acad. Sci. USA *103*, 2474–2479. https://doi.org/10.1073/pnas.0510813103.

63. Anderson, E.L., Baltus, A.E., Roepers-Gajadien, H.L., Hassold, T.J., de Rooij, D.G., van Pelt, A.M.M., and Page, D.C. (2008). Stra8 and its inducer, retinoic acid, regulate meiotic initiation in both spermatogenesis and oogenesis in mice. Proc. Natl. Acad. Sci. USA *105*, 14976–14980. https://doi.org/10.1073/pnas.0807297105.

64. Peng, Y., and Qiao, H. (2021). The application of single-cell RNA sequencing in mammalian meiosis studies. Front. Cell Dev. Biol. *9*, 673642. https://doi.org/10.3389/fcell.2021.673642.

65. Ernst, C., Eling, N., Martinez-Jimenez, C.P., Marioni, J.C., and Odom, D.T. (2019).

Staged developmental mapping and X chromosome transcriptional dynamics during mouse spermatogenesis. Nat. Commun. *10*, 1251. https://doi.org/10.1038/s41467-019-09182-1.

66. Baudat, F., Imai, Y., and de Massy, B. (2013). Meiotic recombination in mammals: localization and regulation. Nat. Rev. Genet. *14*, 794–806. https://doi.org/10.1038/nrg3573.

67. Chen, S., An, G., Wang, H., Wu, X., Ping, P., Hu, L., Chen, Y., Fan, J., Cheng, C.Y., and Sun, F. (2022). Human obstructive (postvasectomy) and nonobstructive azoospermia – insights from scRNA-Seq and transcriptome analysis. Genes Dis. *9*, 766–776. https://doi.org/10.1016/j.gendis.2020.09.004.

68. Acquaviva, L., Boekhout, M., Karasu, M.E., Brick, K., Pratto, F., Li, T., van Overbeek, M., Kauppi, L., Camerini-Otero, R.D., Jasin, M., and Keeney, S. (2020). Ensuring meiotic DNA break formation in the mouse pseudoautosomal region. Nature *582*, 426–431. https://doi.org/10.1038/s41586-020-2327-4.

69. Zhou, R., Wu, J., Liu, B., Jiang, Y., Chen, W., Li, J., He, Q., and He, Z. (2019). The roles and mechanisms of Leydig cells and myoid cells in regulating spermatogenesis. Cell. Mol. Life Sci. *76*, 2681–2695. https://doi.org/10.1007/s00018-019-03101-9.

70. Yu, Y.E., Zhang, Y., Unni, E., Shirley, C.R., Deng, J.M., Russell, L.D., Weil, M.M., Behringer, R.R., and Meistrich, M.L. (2000). Abnormal spermatogenesis and reduced fertility in transition nuclear protein 1-deficient mice. Proc. Natl. Acad. Sci. USA *97*, 4683–4688. https://doi.org/10.1073/pnas.97.9.4683.

71. O'Rand, M.G., Richardson, R.T., Zimmerman, L.J., and Widgren, E.E. (1992). Sequence and localization of human NASP: conservation of a Xenopus histone-binding protein. Dev. Biol. *154*, 37–44. https://doi.org/10.1016/0012-1606(92)90045-i.

72. Kierszenbaum, A.L., and Tres, L.L. (1975). Structural and transcriptional features of the mouse spermatid genome. J. Cell Biol. *65*, 258–270. https://doi.org/10.1083/jcb.65.2.258.

73. Walker, W.H., Sanborn, B.M., and Habener, J.F. (1994). An isoform of transcription factor CREM expressed during spermatogenesis lacks the phosphorylation domain and represses cAMP-induced transcription. Proc. Natl. Acad. Sci. USA *91*, 12423–12427. https://doi.org/10.1073/pnas.91.26.12423.

74. Girault, M.-S., Dupuis, S., Ialy-Radio, C., Stouvenel, L., Viollet, C., Pierre, R., Favier, M., Ziyyat, A., and Barbaux, S. (2021). Deletion of the Spata3 gene induces sperm alterations and in vitro hypofertility in mice. Int. J. Mol. Sci. *22*, 1959. https://doi.org/10.3390/ijms22041959.

75. Zheng, H., Stratton, C.J., Morozumi, K., Jin, J., Yanagimachi, R., and Yan, W. (2007). Lack of Spem1 causes aberrant cytoplasm removal, sperm deformation, and male infertility. Proc. Natl. Acad. Sci. USA *104*, 6852–6857. https://doi.org/10.1073/pnas.0701669104.

76. O'Donnell, L., Nicholls, P.K., O'Bryan, M.K., McLachlan, R.I., and Stanton, P.G. (2011). Spermiation: the process of sperm release. Spermatogenesis *1*, 14–35. https://doi.org/10.4161/spmg.1.1.14525.

77. Lehti, M.S., and Sironen, A. (2017). Formation and function of sperm tail structures in association with sperm motility defects. Biol. Reprod. *97*, 522–536. https://doi.org/10.1093/biolre/iox096.

78. Bao, J., and Bedford, M.T. (2016). Epigenetic regulation of the histone-to-protamine transition during spermiogenesis. Reproduction *151*, R55–R70. https://doi.org/10.1530/REP-15-0562.

79. Ohkura, H. (2015). Meiosis: an overview of key differences from mitosis. Cold Spring Harbor Perspect. Biol. *7*, a015859. https://doi.org/10.1101/cshperspect.a015859.

80. Skinner, M.K. (1987). Cell-cell interactions in the testis. Ann. N. Y. Acad. Sci. *513*, 158–171. https://doi.org/10.1111/j.1749-6632.1987.tb25006.x.

81. Dettin, L., Rubinstein, N., Aoki, A., Rabinovich, G.A., and Maldonado, C.A. (2003). Regulated expression and ultrastructural localization of galectin-1, a proapoptotic beta-galactoside-binding lectin, during spermatogenesis in rat testis. Biol. Reprod. *68*, 51–59. https://doi.org/10.1095/biolreprod.102.006361.

82. Yao, P.-L., Lin, Y.-C., and Richburg, J.H. (2009). TNF alpha-mediated disruption of spermatogenesis in response to Sertoli cell injury in rodents is partially regulated by MMP2. Biol. Reprod. *80*, 581–589. https://doi.org/10.1095/biolreprod.108.073122.

83. Ulisse, S., Farina, A.R., Piersanti, D., Tiberio, A., Cappabianca, L., D'Orazi, G., Jannini, E.A., Malykh, O., Stetler-Stevenson, W.G., and D'Armiento, M. (1994). Follicle-stimulating hormone increases the expression of tissue inhibitors of metalloproteinases TIMP-1 and TIMP-2 and induces TIMP-1 AP-1 site binding complex(es) in prepubertal rat Sertoli cells. Endocrinology *135*, 2479–2487. https://doi.org/10.1210/endo.135.6.7988435.

84. Wang, H., Wen, L., Yuan, Q., Sun, M., Niu, M., and He, Z. (2016). Establishment and applications of male germ cell and Sertoli cell lines. Reproduction *152*, R31–R40. https://doi.org/10.1530/REP-15-0546.

85. Kanatsu-Shinohara, M., Ogonuki, N., Matoba, S., Ogura, A., and Shinohara, T. (2020). Autologous transplantation of spermatogonial stem cells restores fertility in congenitally infertile mice. Proc. Natl. Acad. Sci. USA *117*, 7837–7844. https://doi.org/10.1073/pnas.1914963117.

86. Park, C.J., Ha, C.M., Lee, J.E., and Gye, M.C. (2015). Claudin 11 inter-sertoli tight junctions in the testis of the Korean soft-shelled turtle (Pelodiscus maackii). Biol. Reprod. *92*, 96. https://doi.org/10.1095/biolreprod.114.117804.

87. Mäkelä, J.A., Koskenniemi, J.J., Virtanen, H.E., and Toppari, J. (2019). Testis development. Endocr. Rev. *40*, 857–905. https://doi.org/10.1210/er.2018-00140.

88. Busada, J.T., Chappell, V.A., Niedenberger, B.A., Kaye, E.P., Keiper, B.D., Hogarth, C.A., and Geyer, C.B. (2015). Retinoic acid regulates Kit translation during spermatogonial differentiation in the mouse. Dev. Biol. *397*, 140–149. https://doi.org/10.1016/j.ydbio.2014.10.020.

89. Vernet, N., Dennefeld, C., Rochette-Egly, C., Oulad-Abdelghani, M., Chambon, P., Ghyselinck, N.B., and Mark, M. (2006). Retinoic acid metabolism and signaling pathways in the adult and developing mouse testis. Endocrinology *147*, 96–110. https://doi.org/10.1210/en.2005-0953.

90. Tsai, M.Y., Yeh, S.D., Wang, R.S., Yeh, S., Zhang, C., Lin, H.Y., Tzeng, C.R., and Chang, C. (2006). Differential effects of spermatogenesis and fertility in mice lacking androgen receptor in individual testis cells. Proc. Natl. Acad. Sci. USA *103*, 18975–18980. https://doi.org/10.1073/pnas.0608565103.

91. Heinrich, A., and DeFalco, T. (2020). Essential roles of interstitial cells in testicular development and function. Andrology *8*, 903–914. https://doi.org/10.1111/andr.12703.

92. O'Hara, L., and Smith, L.B. (2015). Androgen receptor roles in spermatogenesis and infertility. Best Pract. Res. Clin. Endocrinol. Metabol. *29*, 595–605. https://doi.org/10.1016/j.beem.2015.04.006.

93. Sofikitis, N., Giotitsas, N., Tsounapi, P., Baltogiannis, D., Giannakis, D., and Pardalidis, N. (2008). Hormonal regulation of spermatogenesis and spermiogenesis. J. Steroid Biochem. Mol. Biol. *109*, 323–330. https://doi.org/10.1016/j.jsbmb.2008.03.004.

94. Meggyes, M., Lajko, A., Fulop, B.D., Reglodi, D., and Szereday, L. (2020). Phenotypic characterization of testicular immune cells expressing immune checkpoint molecules in wild-type and pituitary adenylate cyclase-activating polypeptide-deficient mice. Am. J. Reprod. Immunol. *83*, e13212. https://doi.org/10.1111/aji.13212.

95. Miko, E., Meggyes, M., Doba, K., Barakonyi, A., and Szereday, L. (2019). Immune checkpoint molecules in reproductive immunology. Front. Immunol. *10*, 846. https://doi.org/10.3389/fimmu.2019.00846.

96. Jarow, J.P., and Zirkin, B.R. (2005). The androgen microenvironment of the human testis and hormonal control of spermatogenesis. Ann. N. Y. Acad. Sci. *1061*, 208–220. https://doi.org/10.1196/annals.1336.023.

97. Lau, X., Munusamy, P., Ng, M.J., and Sangrithi, M. (2020). Single-cell RNA sequencing of the cynomolgus macaque

testis reveals conserved transcriptional profiles during mammalian spermatogenesis. Dev. Cell *54*, 548–566.e7. https://doi.org/10.1016/j.devcel.2020.07.018.

98. Tegelenbosch, R.A., and de Rooij, D.G. (1993). A quantitative study of spermatogonial multiplication and stem cell renewal in the C3H/101 F1 hybrid mouse. Mutat. Res. *290*, 193–200. https://doi.org/10.1016/0027-5107(93)90159-d.

99. Fayomi, A.P., and Orwig, K.E. (2018). Spermatogonial stem cells and spermatogenesis in mice, monkeys and men. Stem Cell Res. *29*, 207–214. https://doi.org/10.1016/j.scr.2018.04.009.

100. Lovelace, D.L., Gao, Z., Mutoji, K., Song, Y.C., Ruan, J., and Hermann, B.P. (2016). The regulatory repertoire of PLZF and SALL4 in undifferentiated spermatogonia. Development *143*, 1893–1906. https://doi.org/10.1242/dev.132761.

101. Schmidt, J.A., Avarbock, M.R., Tobias, J.W., and Brinster, R.L. (2009). Identification of glial cell line-derived neurotrophic factor-regulated genes important for spermatogonial stem cell self-renewal in the rat. Biol. Reprod. *81*, 56–66. https://doi.org/10.1095/biolreprod.108.075358.

102. Oatley, J.M., Avarbock, M.R., Telaranta, A.I., Fearon, D.T., and Brinster, R.L. (2006). Identifying genes important for spermatogonial stem cell self-renewal and survival. Proc. Natl. Acad. Sci. USA *103*, 9524–9529. https://doi.org/10.1073/pnas.0603332103.

103. Wang, Z., Xu, X., Li, J.L., Palmer, C., Maric, D., and Dean, J. (2019). Sertoli cell-only phenotype and scRNA-seq define PRAMEF12 as a factor essential for spermatogenesis in mice. Nat. Commun. *10*, 5196. https://doi.org/10.1038/s41467-019-13193-3.

104. Suzuki, H., Ahn, H.W., Chu, T., Bowden, W., Gassei, K., Orwig, K., and Rajkovic, A. (2012). SOHLH1 and SOHLH2 coordinate spermatogonial differentiation. Dev. Biol. *361*, 301–312. https://doi.org/10.1016/j.ydbio.2011.10.027.

105. Chen, W., Zhang, Z., Chang, C., Yang, Z., Wang, P., Fu, H., Wei, X., Chen, E., Tan, S., Huang, W., et al. (2020). A bioenergetic shift is required for spermatogonial differentiation. Cell Discov. *6*, 56. https://doi.org/10.1038/s41421-020-0183-x.

106. Davies, O.R., Maman, J.D., and Pellegrini, L. (2012). Structural analysis of the human SYCE2-TEX12 complex provides molecular insights into synaptonemal complex assembly. Open Biol. *2*, 120099. https://doi.org/10.1098/rsob.120099.

107. Vereecke, G., Defreyne, J., Van Saen, D., Collet, S., Van Dorpe, J., T'Sjoen, G., and Goossens, E. (2021). Characterisation of testicular function and spermatogenesis in transgender women. Hum. Reprod. *36*, 5–15. https://doi.org/10.1093/humrep/deaa254.

108. Kumar, N., and Singh, A.K. (2021). The anatomy, movement, and functions of human sperm tail: an evolving mystery. Biol. Reprod. *104*, 508–520. https://doi.org/10.1093/biolre/ioaa213.

109. Hai, Y., Hou, J., Liu, Y., Liu, Y., Yang, H., Li, Z., and He, Z. (2014). The roles and regulation of Sertoli cells in fate determinations of spermatogonial stem cells and spermatogenesis. Semin. Cell Dev. Biol. *29*, 66–75. https://doi.org/10.1016/j.semcdb.2014.04.007.

110. Al-Attar, L., Noël, K., Dutertre, M., Belville, C., Forest, M.G., Burgoyne, P.S., Josso, N., and Rey, R. (1997). Hormonal and cellular regulation of Sertoli cell anti-Müllerian hormone production in the postnatal mouse. J. Clin. Invest. *100*, 1335–1343. https://doi.org/10.1172/JCI119653.

111. Nicholls, P.K., Stanton, P.G., Chen, J.L., Olcorn, J.S., Haverfield, J.T., Qian, H., Walton, K.L., Gregorevic, P., and Harrison, C.A. (2012). Activin signaling regulates sertoli cell differentiation and function. Endocrinology *153*, 6065–6077. https://doi.org/10.1210/en.2012-1821.

112. Rossi, P., Sette, C., Dolci, S., and Geremia, R. (2000). Role of c-kit in mammalian spermatogenesis. J. Endocrinol. Invest. *23*, 609–615. https://doi.org/10.1007/BF03343784.

113. Liu, S., Chen, X., Wang, Y., Li, L., Wang, G., Li, X., Chen, H., Guo, J., Lin, H., Lian, Q.-Q., and Ge, R.S. (2017). A role of KIT receptor signaling for proliferation and differentiation of rat stem Leydig cells in vitro. Mol. Cell. Endocrinol. *444*, 1–8. https://doi.org/10.1016/j.mce.2017.01.023.

114. Ge, R.S., Dong, Q., Sottas, C.M., Chen, H., Zirkin, B.R., and Hardy, M.P. (2005). Gene expression in rat Leydig cells during development from the progenitor to adult stage. Biol. Reprod. *72*, 1405–1415. https://doi.org/10.1095/biolreprod.104.037499.

115. Huang, L., Xiao, K., Zhang, J., Zhang, P., He, W., Tang, Y., Yang, W., Huang, X., Liu, R., Liang, X., et al. (2021). Comparative transcriptome analysis reveals potential testosterone function-related regulatory genes/pathways of Leydig cells in immature and mature buffalo (Bubalus bubalis) testes. Gene *802*, 145870. https://doi.org/10.1016/j.gene.2021.145870.

116. Cooke, P.S., and Walker, W.H. (2022). Nonclassical androgen and estrogen signaling is essential for normal spermatogenesis. Semin. Cell Dev. Biol. *121*, 71–81. https://doi.org/10.1016/j.semcdb.2021.05.032.

117. Smith, L.B., and Walker, W.H. (2014). The regulation of spermatogenesis by androgens. Semin. Cell Dev. Biol. *30*, 2–13. https://doi.org/10.1016/j.semcdb.2014.02.012.

118. DeFalco, T., Potter, S.J., Williams, A.V., Waller, B., Kan, M.J., and Capel, B. (2015). Macrophages contribute to the spermatogonial niche in the adult testis. Cell Rep. *12*, 1107–1119. https://doi.org/10.1016/j.celrep.2015.07.015.

119. Oatley, J.M., Oatley, M.J., Avarbock, M.R., Tobias, J.W., and Brinster, R.L. (2009). Colony stimulating factor 1 is an extrinsic stimulator of mouse spermatogonial stem cell self-renewal. Development *136*, 1191–1199. https://doi.org/10.1242/dev.032243.

120. Meng, X., Lindahl, M., Hyvönen, M.E., Parvinen, M., de Rooij, D.G., Hess, M.W., Raatikainen-Ahokas, A., Sainio, K., Rauvala, H., Lakso, M., et al. (2000). Regulation of cell fate decision of undifferentiated spermatogonia by GDNF. Science *287*, 1489–1493. https://doi.org/10.1126/science.287.5457.1489.

121. Matson, C.K., Murphy, M.W., Griswold, M.D., Yoshida, S., Bardwell, V.J., and Zarkower, D. (2010). The mammalian doublesex homolog DMRT1 is a transcriptional gatekeeper that controls the mitosis versus meiosis decision in male germ cells. Dev. Cell *19*, 612–624. https://doi.org/10.1016/j.devcel.2010.09.010.

122. Yoshida, S., Sukeno, M., Nakagawa, T., Ohbo, K., Nagamatsu, G., Suda, T., and Nabeshima, Y.I. (2006). The first round of mouse spermatogenesis is a distinctive program that lacks the self-renewing spermatogonia stage. Development *133*, 1495–1505. https://doi.org/10.1242/dev.02316.

123. Seandel, M., James, D., Shmelkov, S.V., Falciatori, I., Kim, J., Chavala, S., Scherr, D.S., Zhang, F., Torres, R., Gale, N.W., et al. (2007). Generation of functional multipotent adult stem cells from GPR125+ germline progenitors. Nature *449*, 346–350. https://doi.org/10.1038/nature06129.

124. Zhao, J., Lu, P., Wan, C., Huang, Y., Cui, M., Yang, X., Hu, Y., Zheng, Y., Dong, J., Wang, M., et al. (2021). Cell-fate transition and determination analysis of mouse male germ cells throughout development. Nat. Commun. *12*, 6839. https://doi.org/10.1038/s41467-021-27172-0.

125. Gao, Y., Xiao, X., Lui, W.-Y., Lee, W.M., Mruk, D., and Cheng, C.Y. (2016). Cell polarity proteins and spermatogenesis. Semin. Cell Dev. Biol. *59*, 62–70. https://doi.org/10.1016/j.semcdb.2016.06.008.

126. Jin, S., Guerrero-Juarez, C.F., Zhang, L., Chang, I., Ramos, R., Kuan, C.-H., Myung, P., Plikus, M.V., and Nie, Q. (2021). Inference and analysis of cell-cell communication using CellChat. Nat. Commun. *12*, 1088. https://doi.org/10.1038/s41467-021-21246-9.

127. Neirijnck, Y., Kühne, F., Mayère, C., Pavlova, E., Sararols, P., Foti, M., Atanassova, N., and Nef, S. (2019). Tumor suppressor PTEN regulates negatively sertoli cell proliferation, testis size, and sperm production in vivo. Endocrinology *160*, 387–398. https://doi.org/10.1210/en.2018-00892.

128. Gnessi, L., Basciani, S., Mariani, S., Arizzi, M., Spera, G., Wang, C., Bondjers, C., Karlsson, L., and Betsholtz, C. (2000). Leydig cell loss

and spermatogenic arrest in platelet-derived growth factor (PDGF)-A-deficient mice. J. Cell Biol. *149*, 1019–1026. https://doi.org/10.1083/jcb.149.5.1019.

129. Basciani, S., Mariani, S., Spera, G., and Gnessi, L. (2010). Role of platelet-derived growth factors in the testis. Endocr. Rev. *31*, 916–939. https://doi.org/10.1210/er.2010-0004.

130. Wijayarathna, R., and de Kretser, D.M. (2016). Activins in reproductive biology and beyond. Hum. Reprod. Update *22*, 342–357. https://doi.org/10.1093/humupd/dmv058.

131. Hedger, M.P., and Meinhardt, A. (2003). Cytokines and the immune-testicular axis. J. Reprod. Immunol. *58*, 1–26. https://doi.org/10.1016/S0165-0378(02)00060-8.

132. Sarkar, O., Mathur, P.P., Cheng, C.Y., and Mruk, D.D. (2008). Interleukin 1 alpha (IL1A) is a novel regulator of the blood-testis barrier in the rat. Biol. Reprod. *78*, 445–454. https://doi.org/10.1095/biolreprod.107.064501.

133. Huleihel, M., and Lunenfeld, E. (2004). Regulation of spermatogenesis by paracrine/autocrine testicular factors. Asian J. Androl. *6*, 259–268.

134. Sorrelle, N., Dominguez, A.T.A., and Brekken, R.A. (2017). From top to bottom: midkine and pleiotrophin as emerging players in immune regulation. J. Leukoc. Biol. *102*, 277–286. https://doi.org/10.1189/jlb.3MR1116-475R.

135. Stuart, T., Butler, A., Hoffman, P., Hafemeister, C., Papalexi, E., Mauck, W.M., 3rd, Hao, Y., Stoeckius, M., Smibert, P., and Satija, R. (2019). Comprehensive integration of single-cell data. Cell *177*, 1888–1902.e21. https://doi.org/10.1016/j.cell.2019.05.031.

136. Korsunsky, I., Millard, N., Fan, J., Slowikowski, K., Zhang, F., Wei, K., Baglaenko, Y., Brenner, M., Loh, P.-R., and Raychaudhuri, S. (2019). Fast, sensitive and accurate integration of single-cell data with Harmony. Nat. Methods *16*, 1289–1296. https://doi.org/10.1038/s41592-019-0619-0.

137. Qiu, X., Mao, Q., Tang, Y., Wang, L., Chawla, R., Pliner, H.A., and Trapnell, C. (2017). Reversed graph embedding resolves complex single-cell trajectories. Nat. Methods *14*, 979–982. https://doi.org/10.1038/nmeth.4402.

138. Krogh, A., Larsson, B., von Heijne, G., and Sonnhammer, E.L. (2001). Predicting transmembrane protein topology with a hidden Markov model: application to complete genomes. J. Mol. Biol. *305*, 567–580. https://doi.org/10.1006/jmbi.2000.4315.

139. Huang, D.W., Sherman, B.T., and Lempicki, R.A. (2009). Systematic and integrative analysis of large gene lists using DAVID bioinformatics resources. Nat. Protoc. *4*, 44–57. https://doi.org/10.1038/nprot.2008.211.

140. Sherman, B.T., Hao, M., Qiu, J., Jiao, X., Baseler, M.W., Lane, H.C., Imamichi, T., and Chang, W. (2022). DAVID: a web server for functional enrichment analysis and functional annotation of gene lists (2021 update). Nucleic Acids Res. *50*, W216–W221. https://doi.org/10.1093/nar/gkac194.

141. Lun, A.T.L., Riesenfeld, S., Andrews, T., Dao, T.P., Gomes, T.; participants in the 1st Human Cell Atlas Jamboree, and Marioni, J.C. (2019). EmptyDrops: distinguishing cells from empty droplets in droplet-based single-cell RNA sequencing data. Genome Biol. *20*, 63. https://doi.org/10.1186/s13059-019-1662-y.

STAR★METHODS

KEY RESOURCES TABLE

REAGENT or RESOURCE	SOURCE	IDENTIFIER
Antibodies		
Rabbit monoclonal [EPR4118] to PGP9.5; dilution: 1:1000	Abcam	Cat# ab108986; RRID:AB_10891773
Rabbit polyclonal to SCP3; dilution: 1:1000	Abcam	Cat# ab15093; RRID:AB_301639
Rabbit monoclonal [EPR3776] to Vimentin; dilution: 1:1000	Abcam	Cat# ab92547; RRID:AB_10562134
Rabbit monoclonal [EPR14335-78] to SOX9; dilution: 1:1000	Abcam	Cat# ab185966; RRID:AB_2728660
Goat Anti-Rabbit IgG H&L (Alexa Fluor® 488); dilution: 1:1000	Abcam	Cat# ab150077; RRID:AB_2630356
Biological samples		
Prepubertal (PRE) buffalo testicular tissue	3 months old	N/A
Pubertal (PERI) buffalo testicular tissue	24 months old	N/A
Chemicals, peptides, and recombinant proteins		
type IV collagenase	Worthington Biochemical Corporation	Cat# LS004188
0.25% Trypsin-EDTA	Sangon Biotech	Cat# E607002-0100
Deoxyribonuclease I (DNase I)	Sigma-Aldrich	Cat# D4527
DMEM	ThermoFisher	Cat# C11995500BT
Fetal Bovine Serum (FBS)	ThermoFisher	Cat# 16140071
Bovine Serum Albumin (BSA)	Sigma-Aldrich	Cat# A9647
0.4% Trypan Blue staining solution	Sigma-Aldrich	Cat# T8154
Critical commercial assays		
Metenyi Dead Cell Removal Kit	Metenyi Biotec	Cat# 130-090-101
10x Chromium Next GEM Single Cell 3′ Reagent Kits v3.1	10x Genomics	Cat# 1000147
Deposited data		
Single-cell RNA-seq data	This paper	GEO: GSE190477
Software and algorithms		
Cell Ranger v 3.1.0	10x Genomics	RRID:SCR_017344
Seurat R package v 3.1.1	[135]	RRID:SCR_016341
Harmony R package v 0.1.0	[136]	RRID:SCR_022206
Monocle R package v 2.22.0	[137]	RRID:SCR_016339
CellChat R package v 1.1.3	[126]	RRID:SCR_021946
TMHMM Server v 2.0	[138]	RRID:SCR_014935
ggplot2 R package v 3.3.6	https://cran.r-project.org/web/packages/ggplot2/index.html	RRID:SCR_014601
GO (DAVID)	[139,140]	RRID:SCR_001881
R version 4.1.3	https://cran.r-project.org/	RRID:SCR_001905
Other		
70 μm cell strainer	NEST	Cat# 258368
40 μm cell strainer	NEST	Cat# 258369
Illumina NovaSeq 6000	Illumina	RRID:SCR_016387
UOA_WB_1 buffalo genome assembly	NCBI	RefSeq assembly accession: GCA_003121395.1

RESOURCE AVAILABILITY

Lead contact

Further information and requests for resources and reagents should be directed to and will be fulfilled by the lead contact, Qiang Fu (gxfuq@gxu.edu.cn).

Materials availability

This study did not generate new unique reagents.

Data and code availability

- All sequencing data in this paper have been deposited at GEO (GSE190477) and are publicly available as of the date of publication. Accession numbers are listed in the key resources table.
- This paper does not report original code.
- Any additional information required to reanalyze the data reported in this paper is available from the lead contact upon request.

EXPERIMENTAL MODEL AND SUBJECT DETAILS

All strategies related to testicular experiments were conducted under CIOMS protocols approved by the Animal Experimentation Ethics Committee (AEEC) of Guangxi University, Nanning, China. The testes of a prepubertal (3-month-old) and a pubertal (24-month-old) normal healthy male buffalo were obtained from the Guangxi Key Laboratory of Buffalo Genetics, Reproduction and Breeding, and from a local slaughterhouse, respectively.

METHOD DETAILS

Buffalo testes sample preparation

Testes from a 3-month-old (prepuberty) and a 24-month-old (puberty) healthy buffalo were washed three times with pre-cooled DPBS to remove the testicular white membrane and epithelium, then instrumented to disrupt testicular tissue and cut into fractions. Single testicular cells were isolated with a two-step enzymatic digestion protocol described previously.[29] Briefly, the cells were incubated with 1 mg/mL type IV collagenase for 8 minat 37°C with a shaker (100 rpm) and washed twice with pre-cooled DPBS. Subsequently, 0.25% Trypsin-EDTA and 0.25 mg/mL DNase I were added and incubated in an incubator at 37°C for 10 min with 15 gentle pulses every 3 min with a blunt tip. Afterward, the digestion was stopped by adding an equal volume of DMEM medium containing 10% FBS. Single testicular cells were obtained by filtering through 70 μm and 40 μm cell strainer, centrifuged at 800 g for 5 min, and washed with pre-cooled DPBS. Then, cells were counted with a hemocytometer and resuspended in phosphate-buffered saline adding 0.4% bovine serum albumin at an adjusted concentration of ~1000 cells/μL for scRNA-seq loading. Cell viability was 92% for prepubertal samples and 86% for pubertal samples using the Metenyi Dead Cell Removal Kit to remove dead cells and cell debris.

10x genome library preparation and sequencing

Single-cell suspensions were obtained in tiny volumes and an equal volume of 0.4% trypan blue staining solution was added for cell quality control, and the available cell concentration was adjusted to the desired concentration (1000–2000 cells/μL). Afterward, the cell suspension was loaded onto a 10x Genomics GemCode Single-cell instrument, and cell capture and library preparation were performed according to the Chromium Next GEM Single Cell 3′ Reagent Kits v3.1 instructions. In addition, high-throughput sequencing of libraries was performed using the PE150 sequencing mode of the Illumina sequencing platform (NovaSeq 6000) at Guangzhou Genedenovo Biotechnology Co., Ltd.

Genome alignment and gene expression quantification

10x Genomics Cell Ranger software (v3.1.0) was used to convert the raw BCL files to FASTQ files, as well as for alignment, and counts quantification. Later, reads with low-quality barcodes and unique molecular identifiers (UMIs) were filtered out and then mapped to the reference genome (UOA_WB_1). In particular, reads uniquely mapped to the transcriptome and intersecting an exon at least 50% were considered for UMI counting. Before quantification, the UMI sequences were corrected for sequencing errors, and valid

barcodes were identified based on the EmptyDrops method.[141] The cell-by-gene matrices were produced by UMI counting and cell barcode calling.

Cell clustering and annotation

The cell-by-gene matrices for each sample were individually imported to Seurat (v3.1.1)[135] for downstream analysis. Primarily, the filtering conditions were as follows: the percentage of the mitochondrial gene was less than 10%, the number of genes that could be detected per cell was 200, and each gene was expressed in a minimum of three cells. Moreover, data was normalized using the LogNormalize method, and the FindVariableFeatures function was used to identify highly variable genes. Samples were integrating using Harmony[136] to remove batch effects and select the first 30 dimensions for analysis. Eventually, tSNE dimensionality reduction was performed using the Seurat function RunTSNE. The Seurat function FindAllMarkers (test used "wilcox" and "min.pct" set to 0.25) was used to calculate marker genes for each cell cluster (Tables S1 and S3). Meiosis-associated and spermiogenesis-related genes were calculated by the Seurat function FindMarkers (min.pct = 0.65, only test genes detected in a minimum fraction of 65% cells in either of the two populations), and the remaining parameters use default settings (Figures 3B, 4B and Table S4). GO and Kyoto Encyclopedia of Genes and Genomes (KEGG) enrichment analyses were performed using DAVID (https://david.ncifcrf.gov/home.jsp).[139,140]

Single-cell trajectory analysis

The single-cell trajectory was analyzed using the matrix of cells and gene expression by the Monocle package in R software (v2.22.0)[137] by the documentation provided. After annotating cell types in Seurat and constructing cell developmental trajectories according to unsupervised analysis methods (DEGs: mean_expression $\geq$0.1 and num_cells_expressed >10), the reverse graph embedding "DDRTree" algorithm was used to dimensionalize the data after downscaling and aligning cells in pseudotime. The cell trajectory plots and heatmap visualization were performed based on the feature values of pseudotime, cell type, and specified genes. All line plots were constructed according to the "loess model" fitted curve in the ggplot2 package, with the horizontal coordinates plotted according to the cell type ordered by the pseudotime value.

Prediction of transmembrane (TM) helices in proteins

TMHMM is an HMM-based (Hidden Markov Model) TM protein prediction tool.[138] The protein sequence was extracted in the FASTA format and calculated by default. The output is presented as following: The length of the amino acid sequence of the protein encoded by the gene is represented by length. ExpAA shows the predicted number of amino acids in the TM helix, and if this score is higher than 18, the protein is the most likely TM or contains a signal peptide structure. First60 refers to the expectation value of amino acids predicted to be TM helices in the first 60 amino acids in the N-terminal protein, predicting the likelihood of the TM helix structure at the N-terminal to be the signal peptide. PredHel predicts the number of TM helices by N-best. The N-best topology determines the final TM result, with "i" indicating that the protein is associated with the inner membrane and "o" indicating that the protein is associated with the extra membrane.

Comparison analysis of PRE- and PERI-derived testicular cells using CellChat

After homologous transformation of buffalo genes to human genes and subsequent analysis, the testicular cell-cell communication network was calculated using the CellChat package in R software (v1.1.3).[126] The expression matrices after standardization of PRE- and PERI-derived cells were extracted from the Seurat objects and then merged by upgrading the CellChat objects after their creation, followed by comparative analysis.

Hematoxylin and eosin staining

The prepared paraffin slices of prepubertal and pubertal testes were deparaffinized, transferred to distilled water for 5 min, stained in hematoxylin for 15 min, and then flushed under flowing water for 3 s in 1% hydrochloric acid solution. Subsequently, the slices were rinsed for 20 min under flowing water, followed by sequential immersion in an alcohol gradient of 70%, 80%, and 90% for 5 min per concentration, and then immersed into 1% eosin staining solution for 10 min. The slices were sequentially dehydrated and made transparent in 95% alcohol (5 min), 100% alcohol I (5 min), 100% alcohol II (5 min), dimethylbenzene

: alcohol = 1 : 1 (10 min), dimethylbenzene I (10 min), dimethylbenzene II (10 min), air-dried, and sealed with coverslips until microscopic examination and image capture.

Immunostaining of buffalo testicular tissue

To improve the permeability of the cell membrane, paraffin sections were deparaffinized, and antigen retrieved (pH 6.0 sodium citrate buffer) and incubated in a 1% Triton X-100-PBST solution for more than 30 min. Thereafter, a 5% BSA blocking solution was poured dropwise onto the sections and sealed at room temperature for 1 h. After incubating each slide overnight at 4°C with the appropriate proportion of diluted primary antibody poured dropwise, the appropriate dilution of fluorescent secondary antibody was added and incubated for 1 hat room temperature, avoiding light, DAPI stained (nuclei), blocked, and observed under a fluorescence microscope.

QUANTIFICATION AND STATISTICAL ANALYSIS

The statistical details of the scRNA-seq data can be found in the figure legends. In Figures 1F, 3B, 4B, S2B–S4B, and S6A and Tables S1, S3, and S4, Wilcoxon rank sum test was performed. The CellChat function netVisual_bubble was used to visualize ligand-receptor interactions (Figure 7D and Table S9). Detailed information on functional enrichment was included in Figures 1G, 5A, and S6E and Tables S2 and S5. The significant level described above was defined as p-value <0.05. In Figures 2E, 3F, 4E, 6D, and S4E, the pseudotime-dependent genes (q-value <0.01) were calculated by trajectory analysis and were for visualization. R (v4.1.3) was used for data processing and visualization.